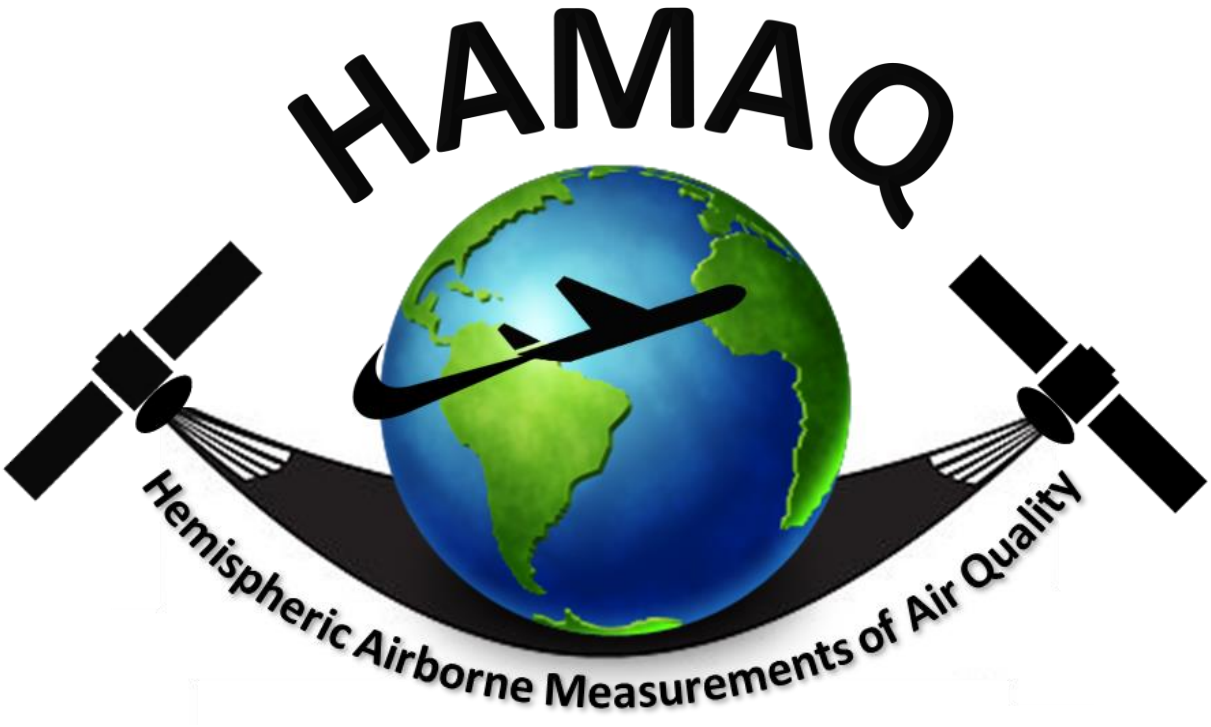

Hemispheric Airborne Measurements of Air Quality (HAMAQ) – North America

Updated December 2025 to reflect deployment location decisions and opportunities for expanded science

Questions should be addressed to Jim Crawford (james.h.crawford@nasa.gov), Laura Judd (laura.m.judd@nasa.gov), and Brian McDonald (brian.mcdonald@noaa.gov)

Abstract

Hemispheric Airborne Measurements of Air Quality (HAMAQ) seeks to advance the understanding and prediction of air quality through the combined use of models and multi-perspective observations from satellites, ground-based observations, and research aircraft. As originally proposed to NASA's Earth Venture Suborbital (EVS-4) solicitation, HAMAQ included airborne sampling under each of the geostationary satellites in the Atmospheric Composition Virtual Constellation (AC-VC) developed under the Committee on Earth Observing Satellites (CEOS). The need to conduct research across the full constellation remains a priority; however, HAMAQ was selected with a reduced budget of $15M and a descoped plan to include only sampling in North America. The science objectives and approach described in this white paper are still relevant to the broader constellation, and partnerships are still in place to continue the pursuit of the larger vision of HAMAQ to also sample in Asia and Europe. For this reason, the NASA-sponsored project will be referred to as HAMAQ-North America. This white paper outlines the science of HAMAQ and the implementation needed to accomplish the North American portion of the effort. HAMAQ plans include two deployments in 2028 over the Mexico City megalopolis in spring and Atlanta, Georgia in summer. The effort will include two aircraft, NASA's B777 for remote sensing and P-3B for in situ sampling. These aircraft will be used to complete the integrated observing system for air quality in combining satellite observations, ground-based monitoring, research aircraft observations, and air quality modeling.

HAMAQ field intensives will serve multiple objectives to include:

- Improving connections between satellites and surface networks through chemically detailed, vertically- and diurnally-resolved measurements.
- Evaluating the magnitude and timing of emissions and their source apportionment to inform inventories and their relationship to satellite column observations.
- Investigating and further develop satellite proxies for air quality.
- Investigating the diversity of factors controlling air quality across multiple urban areas.

This document includes priorities for the airborne observations and modeling that will be needed to accomplish these objectives. Additionally, with the unprecedented prospect to combine up to eight remote sensors on board the B777, opportunities for cross-disciplinary science bridging air quality with Planetary Boundary Layer (PBL) influence and prediction as well as greenhouse gas emissions and carbon cycle impacts are also discussed.

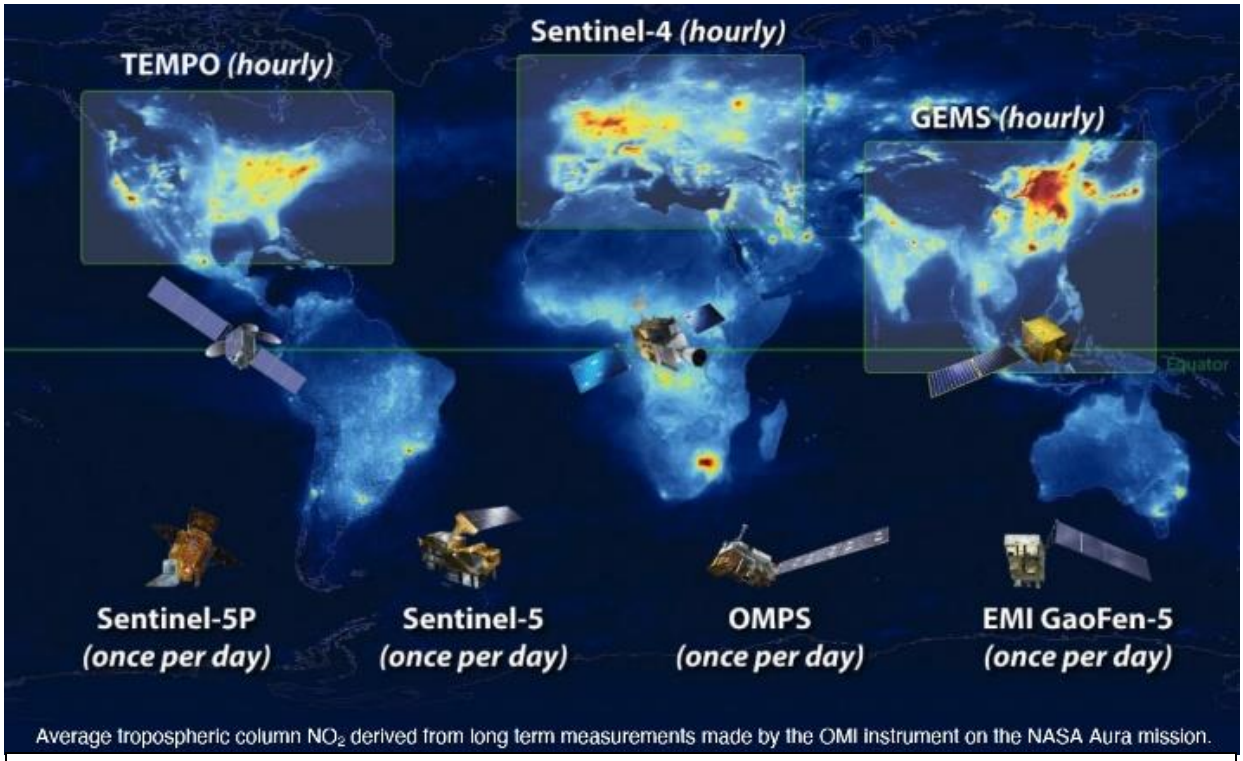

The Atmospheric Composition Virtual Constellation developed under the Committee of Earth Observing Satellites [1].

Introduction

The connection between air pollution and human health calls for continued efforts to improve information on air quality. The Lancet Commission on pollution and health [2] reinforces estimates from the World Health Organization showing that ambient air pollution caused 4.2 million premature deaths in 2019 (8% of all deaths). If unchecked, deaths due to air pollution are expected to increase 50% by 2050. These deaths fall disproportionately on lower-income countries, where pollution accounts for as many as one quarter of deaths. Even for high-income countries, impacts vary with both race and neighborhood income levels, raising further questions regarding how emissions are distributed and how they change over time. Statistically significant increases in mortality have been detected for incremental changes in ozone and fine particulate matter ($PM_{2.5}$) below the current U.S. national standards, demonstrating that there is no threshold below which improving air quality would not provide benefit [3]. There are also general health, economic, and quality of life impacts associated with air pollution [4]. The impact of air quality on agricultural productivity and ecosystem health is particularly noteworthy, e.g., ozone has been estimated to reduce global crop yields by 3-16% [5] with regional impacts being even greater in East Asia [6].

In recognition of these issues, an international constellation of air quality observing satellites, conceived and organized through the Committee on Earth Observation Satellites (CEOS) [1], is now coming to fruition to provide a space-based view at unprecedented temporal and spatial resolution. This constellation includes three geostationary satellite instruments dedicated to hourly daytime observations at high spatial resolution across much of the populated regions of the Northern Hemisphere:

- the Geostationary Environment Monitoring Spectrometer (GEMS) launched by Korea over Asia in February 2020 [7];
- the Tropospheric Emissions: Monitoring of Pollution (TEMPO) instrument launched by NASA over North America in April 2023 [8];
- the Sentinel-4 satellite launched by the European Space Agency (ESA) over Eiurope in July 2025 [9].

These instruments are augmented by global coverage from low-Earth orbiting satellites like ESA's TROPOMI (TROPOspheric Monitoring Instrument) on Sentinel-5P [10], NOAA-NASA OMPS (Ozone Mapping and Profile Suite Instrument), and the most recently launched Sentinel-5 and Global Observing SATellite for Greenhouse gases and Water cycle (GOSAT-GW) [90] missions in summer 2025. These and other satellites observing trace gases and aerosols will provide an unprecedented view of air quality over the major population centers in the Northern Hemisphere.

The constellation provides an ideal framework for international cooperation to better understand air quality from local-to-global scales. This includes data sharing, validation, intercomparison, and interpretation. To be successful, these satellite observations must be integrated with ground and airborne measurements and models to realize their full potential for assessing the factors controlling air quality over specific regions and providing actionable information to decision makers. This requires an **integrated observing system** for air quality as depicted in Figure 1.

In anticipation of the constellation, NASA field campaigns have already provided opportunities to put multi-perspective observations into place to replicate the integrated observing system. These include DISCOVER-AQ (Deriving Information on Surface conditions from COlumn and VERtically resolved observations relevant to Air Quality) [11] during 2011-2014 and the KORUS-AQ (Korea-United States Air Quality) field study [12] in 2016. Several smaller studies have also

implemented subsets of the observing system (e.g., [13-16]). More recently, campaigns have been conducted in coordination with GEMS, e.g., SIJAQ and ASIA-AQ, and in coordination with TEMPO, e.g., AEROMMA and STAQS.

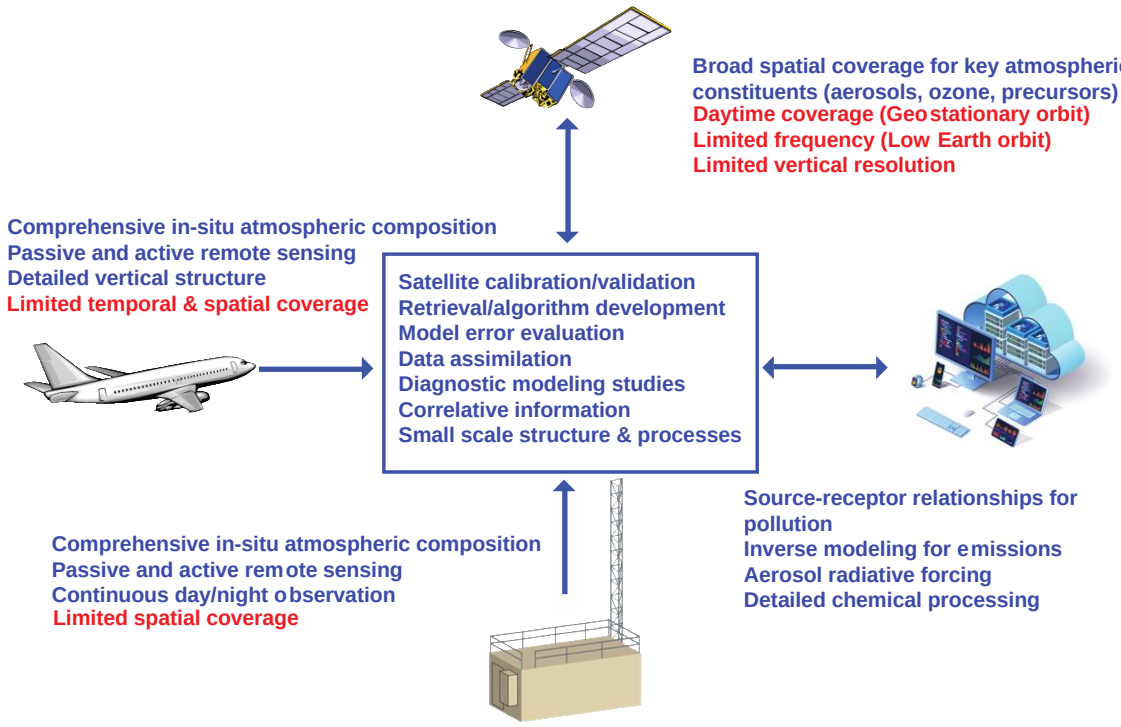

Figure 1. Schematic of the integrated observing system for air quality describing the strengths and weaknesses of each observational perspective and how their complementarity benefits models and improves understanding of the factors controlling air quality.

Building upon these efforts, NASA's Earth Venture Suborbital Program has provided funding for observations over North America as part of a project called Hemispheric Airborne Measurements of Air Quality (HAMAQ; pronounced "hammock"). Flights over North America will provide an important opportunity to exercise the fully integrated observing system under TEMPO. Described in more detail below, HAMAQ will employ a two aircraft sampling strategy with the NASA B777 for remote sensing and the NASA P-3B for *in situ* observations. These aircraft will be deployed to the Mexico City megalopolis in spring 2028 followed by Atlanta, Georgia in summer 2028. Specific sampling considerations for these locations will be discussed below.

HAMAQ Science Goal and Objectives

The long-term vision for HAMAQ extends beyond just the planned deployments over North America and includes objectives that broadly apply to observations across the air quality constellation. This white paper also serves as a tool for planning other potential opportunities to fly in Asia under GEMS and Europe under Sentinel-4.

The goal of HAMAQ is to advance the integrated observing system for air quality through targeted airborne observations over priority areas in coordination with the geostationary air quality satellite constellation and local monitoring to improve forecasting and inform policy.

To accomplish this goal, HAMAQ will focus on four science objectives and associated science questions are discussed below.

Objective 1: Improve connections between satellites and surface networks through chemically detailed, vertically- and diurnally-resolved measurements.

Questions: What factors limit our ability to effectively integrate satellite and ground-based observations (e.g., diurnal changes in emissions and vertical mixing and other uncertainties in satellite retrievals at the urban to regional scale)?

Geostationary air quality observations are powerful in their ability to provide high time and spatial resolution but also uniquely challenged in that retrievals require reliable information on the changing vertical structure of atmospheric composition throughout the day. These retrievals also have uncertainties driven by surface reflectivity, clouds, and aerosols [17-20]. Systematically repeated *in situ* airborne profiling has proven critical to fully interpret the relationship between column-integrated and surface concentrations of air pollutants. DISCOVER-AQ offered the first opportunity to continuously observe diurnal changes in column density of trace gases against surface *in situ* measurements by placing Pandora spectrometers at air quality monitoring sites to provide direct-sun remote sensing of trace gas columns. Diverse behaviors were observed across the DISCOVER-AQ deployments, demonstrating the value of campaigns in multiple urban locations. Figure 2 shows an example from Colorado of the complex relationship between surface and column conditions. On the left, diurnal statistics are compared at three locations for Pandora column observations and surface measurements during the one-month field study. Early morning reductions in surface NO_2 at LaCasa (in Denver) versus large increases in the column abundance suggest very strong vertical mixing as emissions continue to accumulate (right panel). The diurnal trend in column abundance is similar for the I-25 site (also in Denver), but surface NO_2 is greater with less diurnal variability for this roadside location with high traffic density. For Golden (west of Denver at the edge of the foothills of the Rocky Mountains), column NO_2 increases throughout

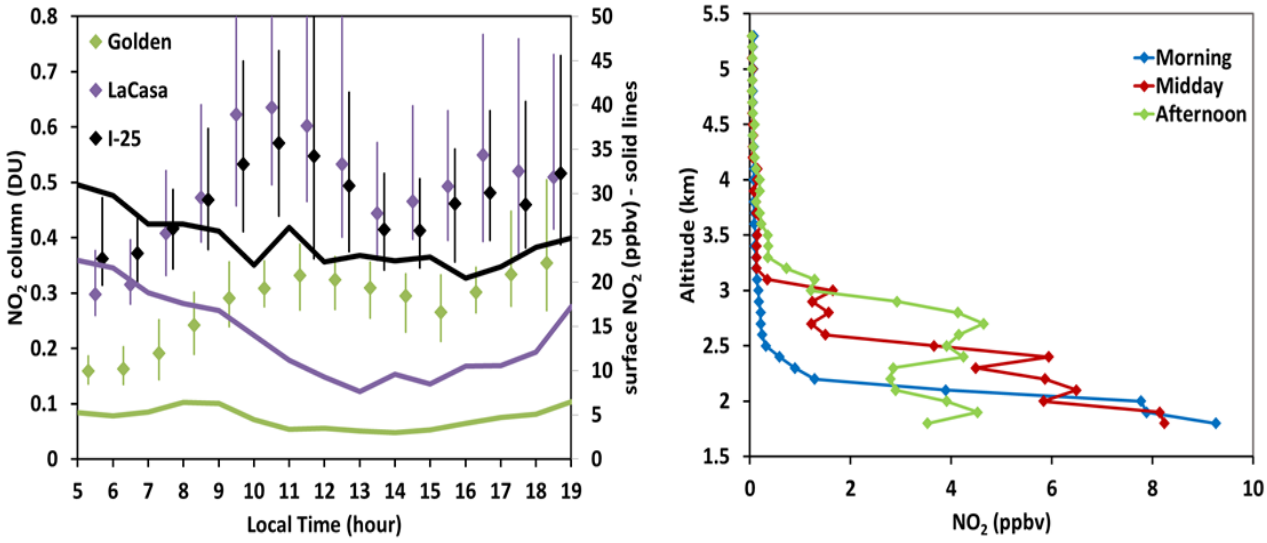

Figure 2. (Left) Diurnal trends in NO_2 column density (median and interquartile range) and surface situ NO_2 (lines) at three sites during DISCOVER-AQ Colorado. (Right) Average airborne in situ profiles over the LaCasa site demonstrating diurnal changes in column density and NO_2 gradients within the boundary layer [21].

the day as emissions from Denver are transported toward the mountains, but this is not evident in the surface observations. Continued documentation of these types of behaviors in surface and column quantities is needed to ensure the proper interpretation of satellite observations. For instance, diurnal changes in the vertical profile must be accounted for to enable accurate retrievals of the hourly variation in column densities observed from geostationary orbit.

The influence of vertical distribution on trace-gas columns becomes even more complex when considering multiple compounds. Figure 3 compares statistics for the vertical distributions of NO_2 and CH_2O observations collected during KORUS-AQ in Seoul. Airborne *in situ* profiles indicate progressively deeper mixing throughout the day accompanied by dilution of near-surface NO_2, which is directly emitted. By contrast, CH_2O is produced photochemically and is not observed to be depleted near the surface. Increased production of CH_2O as the boundary layer deepens and photochemistry becomes more active drives different column to surface relationships than for NO_2. Exploring the diversity in diurnal behavior in trace gas column densities and vertical distributions across more locations and conditions will be critical to interpretation of the data from the satellite constellation for use in the integrated observing system. Figures 2 and 3 offer examples of how column and surface behavior can differ substantially, but they should not be considered typical. Changes in emissions, chemical production and loss, vertical mixing, and advection all contribute to differences in surface to column behavior. These factors depend on location and contemporaneous meteorological conditions. Detailed sampling of strong spatial and temporal gradients is needed to investigate these differences and evaluate their representation in air quality models which are used to generate a priori conditions for satellite retrievals.

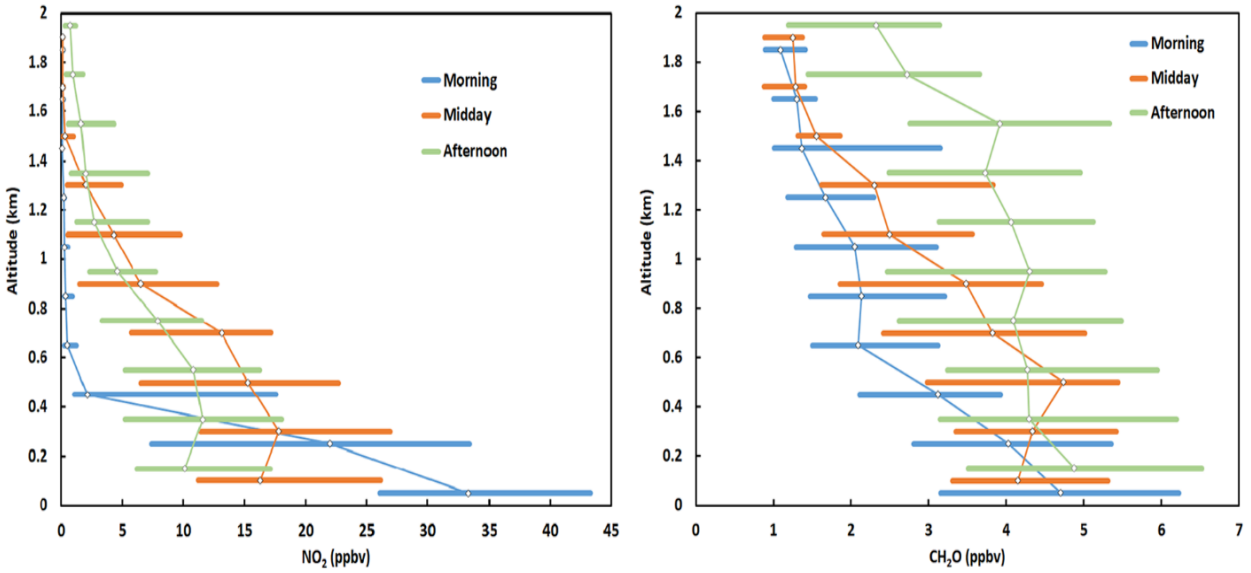

Figure 3. Diurnal statistics (median and interquartile range) for vertical profiles of NO_2 (left) and CH_2O (right) over Seoul during KORUS-AQ [22].

Aerosol optical depth (AOD) is the space-based retrieved quantity available to inform surface concentrations of $PM_{2.5}$. This must be derived using a combination of observations and models to determine the AOD-$PM_{2.5}$ relationship. Studies of diurnal variations of co-located measurements of column AOD and surface $PM_{2.5}$ reveal large variability in this relationship [23-25] that is sensitive to the vertical distribution of aerosols, aerosol composition and ambient water vapor or relative humidity, since different aerosol species and particle sizes have different hygroscopic properties and mass to optical conversion efficiencies. These factors make the interpretation of remote-sensing measurements of AOD to surface $PM_{2.5}$ concentrations difficult. Figure 4 shows examples of daytime variations of AOD with $PM_{2.5}$ and column water vapor at the same time and location. These data illustrate that AOD can show correlation with neither $PM_{2.5}$ nor water vapor (case 1), with one of them (case 2), or both (case 3). HAMAQ will provide detailed vertical profiles of aerosol composition and physical/optical properties across the diurnal cycle that are critical for explaining AOD and $PM_{2.5}$ relationships and addressing how and when AOD can be used to inform surface $PM_{2.5}$ air quality.

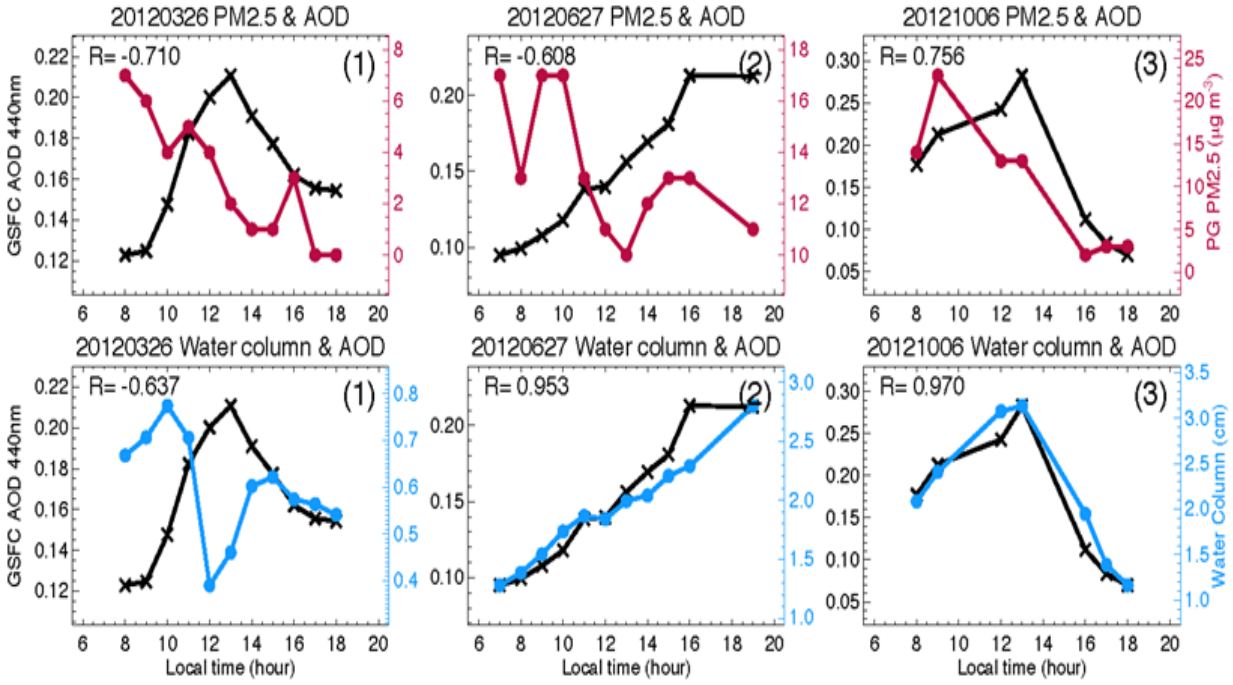

Figure 4. Daytime variations of AERONET AOD and column water vapor and EPA $PM_{2.5}$ near Washington, DC in 2012.

Objective 2: Evaluate the magnitude and timing of emissions and their source apportionment to inform inventories and their relationship to satellite column observations.

Questions: Do emission inventories adequately explain observed spatial and temporal distributions of NO_2, CH_2O, and SO_2? What do detailed observations, including speciated hydrocarbons and tracers, indicate about emissions from anthropogenic and natural sources in each target region?

Emissions are critical to understanding drivers of air pollution and are developed from activity and ground-based information (bottom-up) that is unrelated to observations of the resulting atmospheric concentrations. Space-based observations provide an important top-down constraint for evaluating bottom-up inventories. *In situ* observations are critical to provide detailed composition needed for source apportionment that cannot be measured via satellite instruments. Aircraft observations are also ideal for obtaining this information from a regional perspective to observe composition affected by a combination of sources.

The secondary nature of ozone and $PM_{2.5}$ pollution requires an understanding of the precursor emissions and chemistry that determine their distributions. This understanding is fundamental to any successful strategy to improve air quality through targeted reduction of emissions. Several crucial ozone and $PM_{2.5}$ precursors will be observed by the satellite constellation including NO_2 (a proxy for total nitrogen oxides, NO_x) and CH_2O (a proxy for volatile organic carbon species, VOC). Field campaigns routinely reveal deficiencies in emissions that have implications for model prediction of ozone and $PM_{2.5}$. During KORUS-AQ, aircraft *in situ* profiles of composition compared to model simulations revealed important deficiencies in both the NO_x and aromatic VOC inventories that resulted in large underestimates in simulated ozone production [26]. These discrepancies were also relevant to $PM_{2.5}$ given the high potential for these emissions to form the secondary inorganic and organic aerosol that dominated aerosol composition during KORUS-AQ [27]. In an air quality modeling study from DISCOVER-AQ [28], the observed ozone distribution was reproduced by the model despite overprediction of NO_2 and underprediction of CH_2O. In a second simulation, well-posed improvements included a reduction in traffic emissions of NO_x and an increase in VOC emissions from vegetation. The resulting predictions of ozone were similar to the original model output; however, in this case the precursor fields were in much better agreement. This study demonstrates a classic example of getting the right answer for the wrong reason, highlighting the importance of representing precursors and their emissions correctly in air quality models.

While *in situ* profiles provide a quick assessment of the magnitude of emissions, mapping of precursors with airborne remote sensing provides additional value for understanding the spatial distribution and timing of emissions. Figure 5 shows distributions of NO_2 and CH_2O over the Seoul Metropolitan Area for four consecutive raster maps collected from morning to late afternoon on a single day. The differences between each consecutive map highlights the importance of having geostationary observations to provide multiple views per day. High-resolution airborne observations provide detailed information relating not only to emissions but also chemistry and transport. In this example, early morning distributions show distinct sources. Later in the day, chemistry and transport lead to a convergence in the NO_2 and CH_2O distributions. Through both

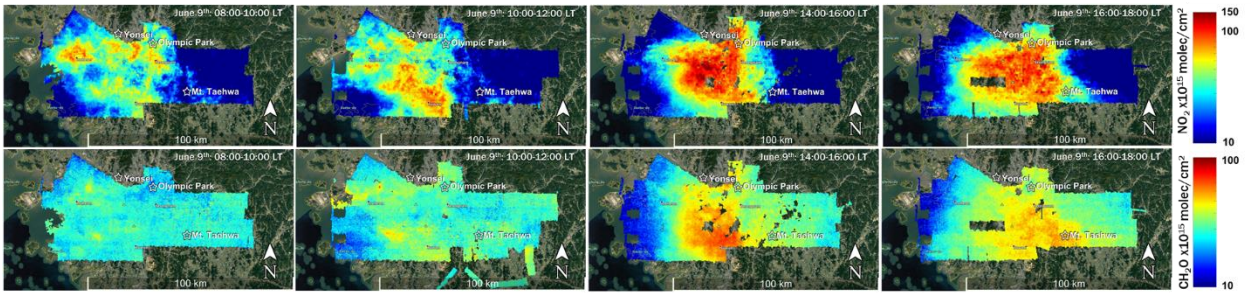

Figure 5. Airborne mapping of NO_2 and CH_2O column densities across the Seoul Metropolitan Area on June 9, 2016 [22].

direct comparison with models and use of model inversions, aircraft *in situ* and remote sensing observations can provide an excellent assessment of emissions and their air quality impacts. During KORUS-AQ, remote sensing observations also contributed to an assessment of SO_2 point source emissions [29] and top-down estimation of anthropogenic VOC emissions [30, 31].

Evaluating emissions inventories also requires observations of more than just those species observed by satellites. Global emission inventories struggle to properly represent observations of speciated VOCs, while regional inventories developed by local expertise appear to better agree with atmospheric observations [32]. Satellite-observed CH_2O suggests that VOC emissions have been rapidly changing in Asia [33]. Comprehensive *in situ* observations of atmospheric composition will be critical for source apportionment and fingerprinting of diverse emission sources. For example, exploring discrepancies in CH_2O distributions will require speciated VOC measurements to differentiate and quantify biogenic and various anthropogenic source contributions. The relative roles of VOC emissions and oxidation rate (OH production) will also have to be carefully considered in examining CH_2O distributions [34]. HAMAQ will map satellite observed precursors (e.g., NO_2, CH_2O, and SO_2) at high spatial resolution at different times of day and provide comprehensive observations of *in situ* composition needed to better understand emissions and source apportionment.

Objective 3: Investigate and further develop satellite proxies for air quality.

Questions: Can satellite data provide useful information on surface air quality for ozone and $PM_{2.5}$ either directly or through the use of precursor gases (e.g., CH_2O as a proxy for ozone or organic aerosol; the product of NO_2 and CH_2O as an indicator of ozone production rates)? Can satellite observations be used to identify gaps in ground monitoring?

Satellite observations provide limited information on surface air quality for species such as ozone where sensitivity to the lowest part of the atmosphere is limited. There are ongoing efforts to develop satellite retrievals for lower tropospheric ozone [35-37], but the quality of these products must be determined. TEMPO is the only instrument in the constellation that will provide a 0-2 km ozone product. To improve the interpretation of satellite observations for near-surface conditions, other relationships (proxies) need to be explored, developed, and verified.

One such proxy that emerged from analysis of previous campaigns is correlation between column CH_2O and surface ozone [38,39]. The potential value of this proxy has been demonstrated for both temporal and spatial variations in the relationship. Figure 6 shows how variations at a single location over time show a tendency toward higher CH_2O on high ozone days. While the quality of the relationship is not robust enough to predict ozone directly, long-term averaging of satellite CH_2O distributions might be useful for evaluating the placement of ozone monitors by identifying where increased ozone exposure is most likely to occur. Reevaluating networks becomes more important as precursor emissions continue to change [40,41]. This proxy has not yet been applied from any space-based observations, but geostationary satellites may have sufficient temporal and spatial resolutions to realize its potential for mapping surface ozone gradients. Pandora spectrometers will play an increasing role having recently been improved to enable a reliable retrieval of CH_2O [42] to help identify regions where satellites could apply this proxy. Additional complicating factors include the need to consider Ox (O_3+NO_2) in high NOx environments and possible drifting in the relationship as seasonal VOC sources and photochemical lifetimes vary

[39]. Developing a proxy for surface ozone also provides the opportunity to expand the analysis in inequalities in pollution exposure that have been largely based on a combination of satellite and aircraft mapping of NO_2 columns [43,44]. Further testing of this proxy across a wider range of conditions will be possible during HAMAQ through airborne remote sensing of CH_2O and ozone over domains with dense surface ozone monitoring networks.

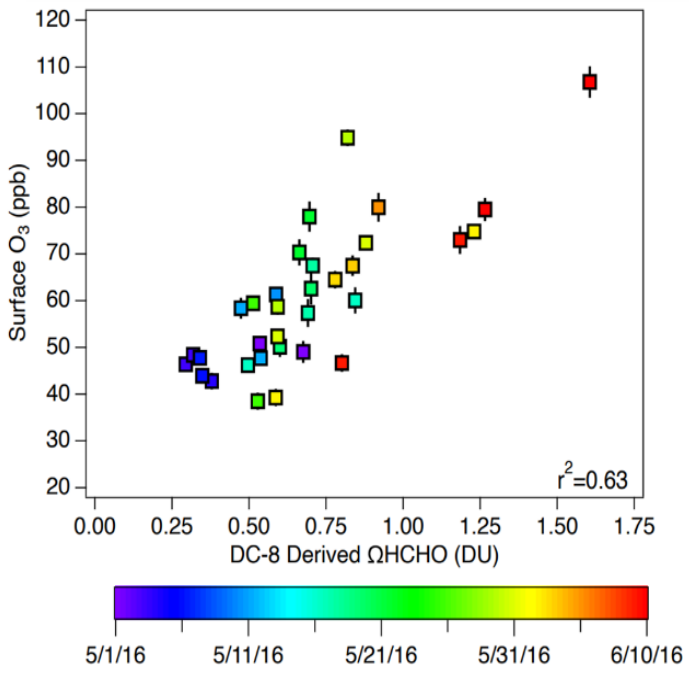

Figure 6. Correlation of surface ozone with airborne in situ CH_2O in Seoul [39].

Preliminary work has shown additional promise for CH_2O columns as a proxy for organic aerosol (OA) [45,46], a major component of $PM_{2.5}$ [47]. This relationship varied depending on whether an environment was dominated by anthropogenic, biogenic, or biomass burning VOC emissions. With the availability of geostationary satellite observations of other aerosol precursors (e.g., NO_2 and SO_2), HAMAQ will provide comprehensive observations of trace gas precursors and aerosol composition to study and promote uses of satellite data for better understanding surface $PM_{2.5}$ concentrations and composition.

A popular satellite proxy is the ratio of column densities for formaldehyde and NO_2 (CH_2O:NO_2). This quantity was first suggested in 2004 as an indicator of the relative sensitivity of ozone formation to NO_x (CH_2O:NO_2 > 1) and VOCs (CH_2O:NO_2 < 1) during summer [48]. Thus, information on the broad distribution of this ratio has been considered useful to developing more effective emission control strategies. Subsequent work refined the quantitative use of the ratio, showing that there was also a substantial transition zone (1 < CH_2O:NO_2 < 2) for which neither NO_x nor VOC sensitivity dominates [49]. This ratio has been applied to examine ozone formation sensitivity in different parts of the world [50-55]. All of these analyses are based on monthly average observations from low earth orbiting satellites for a single time of day in the early afternoon. In anticipation of geostationary observations, DISCOVER-AQ provided the first chance to evaluate the diurnal and daily behavior in this ratio [56]. The use of this ratio was found to be complicated by: 1) a larger transition zone that varies by location, 2) large changes with time of day, and 3) distinctly different ratios under polluted conditions relative to the average. The diurnal changes in the vertical distributions for the two species shown in Figure 3 further demonstrate the complication with this proxy from the column perspective as associated ozone production sensitivity varies significantly with altitude. Recent work highlighted additional uncertainties in CH_2O:NO_2 associated with retrievals, spatial resolution, chemistry, and vertical distributions and introduced a promising new proxy for ozone production rates using the product of NO_2 and CH_2O [57]. These findings challenge the previous use of monthly average distributions and suggest that more analysis is needed to determine how this ratio can be beneficially applied to the development of control strategies. HAMAQ will

provide an opportunity to look deeper into the use of CH_2O and NO_2 to understand ozone chemistry and broaden the conditions for testing proxies for surface ozone concentrations and production rates.

Objective 4: Investigate the diversity of factors controlling air quality across multiple urban areas.

Questions: What are the common and unique issues underlying the distribution and trends in ozone and $PM_{2.5}$ across different locations? How can geostationary observations improve prediction of changes related to future mitigation measures? What is the role of changes in urban characteristics on meteorology and air quality, and how does this impact interpretation of geostationary satellite retrievals?

The first three HAMAQ objectives focus heavily on the constituents that can be measured from space, but the contextual setting and how it may influence the use of satellite observations will be a particularly valuable contribution of HAMAQ. This requires investigation of the detailed composition of pollution and the meteorological conditions affecting chemistry as well as satellite observability needed to improve air quality models. Specific local factors related to emissions, meteorology, and geography contributed to observed violations of air quality for all four locations visited by DISCOVER-AQ. Petrochemical emissions played a unique role in Houston [65,66]. Agriculture and livestock emissions were much more important in California's Central Valley [67]. In Colorado, emissions from traffic in the Denver area, power generation and industrial activity just outside the city, oil and gas exploration to the east, and feedlots to the northeast all contributed to the local air quality outcomes [68-70]. Conditions in Maryland and Houston were exacerbated by the influence of coastal sea breezes [71,72] while terrain influences were more important in California and Colorado [73,74]. During KORUS-AQ in South Korea, the importance of aromatic VOC emissions to ozone chemistry resulted in changes to the emissions inventory and to air quality models that had lacked sufficient treatment of their chemistry [27].

Regional differences may also affect satellite data interpretation. For instance, detailed VOC measurements can help resolve whether the balance between anthropogenic and biogenic emissions (Objective 2) affects the satellite proxies that rely on CH_2O observations (Objective 3). The relative importance of non-combustion VOC sources (solvents, paints, fragrances, cooking, urban vegetation) is increasing in urban areas as emissions from traditional sources (traffic, power plants) decrease [75-79]. Traffic emissions may be a large source of ammonia in urban regions that contribute to $PM_{2.5}$ formation [80]. Aircraft observations will significantly contribute to efforts to improve the chemical mechanisms that describe ozone and $PM_{2.5}$ formation from these sources. Satellite retrievals of NO_2 from polar orbiters have been exploited to inform oxidant chemistry in cities [81] and geostationary observations combined with aircraft observations will facilitate this understanding at unprecedented spatial and temporal scales.

Emissions of precursors generally have different distributions than ozone and $PM_{2.5}$, confounding the use of remote sensing data for inference of secondary pollutant production. Figure 7 provides an example of the power of comprehensive remote sensing observations over Houston, Texas during TRACER-AQ (TRacking Aerosol Convection ExpeRiment - Air Quality) in 2021. Concurrent observations of column CH_2O, NO_2, aerosol optical depth (AOD), and near-surface ozone mapped from aircraft several times per day over an urban area can facilitate a deeper understanding of connections between surface monitors, *in situ* aircraft observations, and satellite retrievals. Afternoon conditions from a high ozone day (Fig. 7) illustrate both similarities and differences in precursor distributions and secondary pollution indicated by near-surface ozone and AOD. In addition to AOD, the vertical distribution of aerosols from active remote sensing can also inform variability in boundary layer depth that can be related to urban characteristics such as the heat island effect [82] using a co-located surface temperature measurement planned for upcoming campaigns. While detailed *in situ* observations are not available in this case, the combination of airborne remote sensing and in situ observations during HAMAQ will provide the ability to interpret differences in ozone chemistry and pollution sources needed to help explain these distributions. Evidence of transport observed from satellites must be interpreted with care using detailed aircraft and ground-based observations. During KORUS-AQ, a long-range transport event was associated with a large increase in local $PM_{2.5}$ measured at monitoring sites. This increase was poorly captured by models and was overly attributed to China. This event was observed by ground-based (AERONET) and satellite AOD, and model improvements based on aircraft data were made to the treatment of aerosol optical properties [83] and chemical production [84] to better account for local chemical production vs. long-range transport of pollution, which resulted in a shift in aerosol composition. Better understanding this balance between local and transported impacts is particularly important for decision-making. Such improvements also lead to better fusion of satellite and model observations to infer $PM_{2.5}$ composition (e.g., MAIA). HAMAQ will employ the integrated observing system for air quality to explore diversity in geography, meteorology, emissions, and other factors that can inform models used to demonstrate how decisions affect air quality and evaluate the role of geostationary observations to expand interpretation of these diverse factors to other regions.

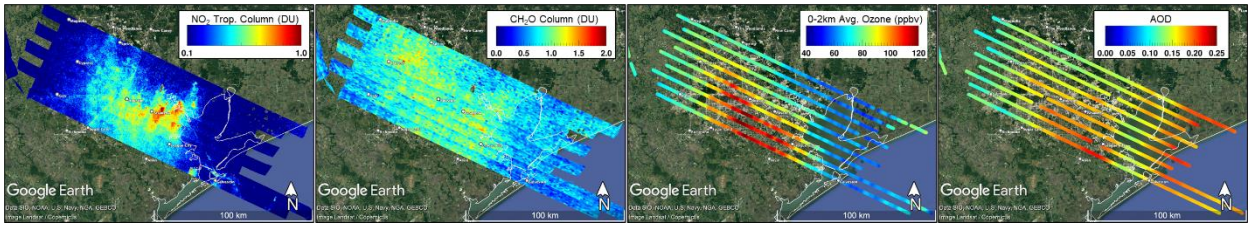

Figure 7. September 9th, 2021 afternoon raster over Houston, Texas for a) NO_2, b) CH_2O, c) Lidar ozone (0-2 km), d) Lidar AOD (532nm)

Science Implementation

To be successful, HAMAQ will need to employ each component of the integrated observing system for air quality as described below.

Satellite Constellation – HAMAQ is dependent on the successful launch and operation of the satellites in the air quality constellation. Specifically, TEMPO will be the primary focus of deployments conducted under NASA's Earth Venture Suborbital program. HAMAQ may also benefit the Multi-Angle Imager for Aerosols (MAIA) instrument (expected launch in 2026) which includes Atlanta as a primary target area and Mexico City as a secondary target area (https://maia.jpl.nasa.gov/mission/#target_areas). GOSAT-GW [90] also has a focus mode that could be leveraged for higher resolution information if coordination allows.

Surface Networks – HAMAQ science will rely heavily on existing air quality monitoring networks. These ground measurements provide a critical element of continuity, providing information at all times of day and under all conditions, unlike research flights and satellite observations. Connecting scientifically to the surface observations used by regulators is fundamental to the success of the observing system. An additional important element relates to ground-based remote sensing by Pandora spectrometers, AERONET sunphotometers, and other ground-based instruments already operating in each visited domain.

Airborne Observations – Airborne observations will be at the center of HAMAQ's contribution to the integrated observing strategy. Each deployment will use a combination of two aircraft: the NASA B777 for mapping with remote sensors and the NASA P-3B for *in situ* sampling and profiling of the lower atmosphere. Airborne remote sensing over the targeted domains will focus on constituents visible from space but at higher spatial resolution. HAMAQ also welcomes international and interagency partners to contribute and fly instruments of opportunity given the capacity of the B777. HAMAQ will also open cross-disciplinary science opportunities to investigate Planetary Boundary Layer (PBL) influence on air quality and the intersection between air quality and climate through greenhouse gas emissions. *In situ* observations will require an extensive payload to characterize detailed trace gas and aerosol composition including satellite-observed constituents along with comprehensive measurements that provide valuable context on the sources, chemistry, and meteorological conditions that contribute to emissions and air quality outcomes. These measurements are outlined in Table 1 of the Appendix. The NASA P-3B is capable of hosting a payload that would include all priority 1 *in situ* measurements with possible room for some priority 2 measurements depending on the instrumentation selected. Priority 3 *in situ* measurements would only be included if they could be provided by an instrument already addressing higher priority measurements.

Modeling and Analysis – HAMAQ will require a suite of models to support all phases of the project: preparation, execution, and post-mission analysis. These models will range from global to regional to local scales as well as observation-based 0-D chemical box modeling constrained by airborne observations. Models will need to employ various methods (e.g., tagged tracers, data assimilation, and inverse modeling) to provide forecasts for flight planning and post-mission investigation of vertical structure of atmospheric composition, satellite retrievals, emissions inventories, and identification of source contributions to observed abundances of primary and secondary pollutants. Satellite retrievals, aircraft observations, and surface measurements all will be used to quantitatively evaluate the models leading to the improvement of air quality forecasts. Data assimilation of AOD and trace gases is desired to help identify deficiencies in emissions and

model processes. Specific model requirements are listed in Table 2 in the Appendix. Given the high applied value of HAMAQ observations, it is expected that modeling will also be pursued by local agencies and scientists.

HAMAQ Airborne Deployments – Building upon successful sampling strategies developed during previous air quality studies, HAMAQ will conduct flights over two metropolitan areas: the Mexico City megalopolis and Atlanta, Georgia. Figure 8 shows the deployment domain for each location including the monthly average distribution of NO_2 observed by TEMPO during the expected month of deployment, current ground-based monitoring sites, and a potential domain for remote sensing (indicated by the white box). Each deployment will perform airborne sampling on at least 8 days to ensure observations for a sufficient variety of meteorological conditions and range of air quality severity spanning clean to polluted conditions. The white box represents the areal extent of remote sensing that can be mapped three times per day by the B777. The dimensions of the box have been optimized based on an average ground speed of 400 kts to conserve spatial resolution of products from previous missions and an expectation of about 8 hours of flight time. *In situ* sampling by the P-3B will balance the need for profiling the lower atmosphere with sampling more broadly to examine regional conditions upwind and downwind of areas in violation of air quality standards. Aircraft symbols in Figure 8 show locations for possible P-3B low approaches to allow *in situ* profiling to extend to the surface. Integrated sampling by these two aircraft will provide a strong scientific basis for the interpretation of satellite observations and the application of satellite-derived information about air quality across the broader domain. Final placement of the B777 remote sensing domain and flight lines for the P-3B will be designed in full cooperation with local scientists, environmental agencies, and the HAMAQ Science Team.

The contrast between Mexico City and Atlanta is evident in the TEMPO NO_2 distributions shown in Figure 8. Mexico City is characterized by strong containment of emissions in a basin that is surrounded by high mountainous terrain. Evidence of this containment shows up in the TEMPO observations as a strong, localized enhancement in NO_2 that stands out against the surrounding region. The NO_2 levels in Atlanta are substantially less in magnitude, and the NO_2 distribution shows a much more gradual transition with the surrounding region given the absence of large mountains or bodies of water that disrupt flow patterns.

The Mexico City Megalopolis represents the most populated and polluted domain within the TEMPO field of regard and is largely isolated from transboundary influences. Despite improvements in historical air quality conditions, this region has seen little progress in reducing ambient ozone and $PM_{2.5}$ in the last decade [85]. There are multiple factors contributing to this lack of progress [86] including continued urban expansion of the Mexico City Metropolitan Area into the larger surrounding Megalopolis with a population of more than 30 million, complex topography surrounding the cities influencing transport patterns, and a variety of industrial sources, agricultural burning, and volcanic activity. The scarcity of measurements outside the metropolitan area leaves an open question of the influence and impacts of unreported emissions from the nearby urban and rural regions. HAMAQ would aim for the March 2028 timeframe for deployment which coincides with the dry season, elevated ozone values above the US EPA NAAQS most afternoons and largely cloud-free climatology (Figure 9). While ozone season extends beyond March with interest in April-May, satellite observations of clouds from GOES-16 ABI show strong trends toward cloudy afternoons after March. Mexico City and its surrounding industrial areas offer the highest resolution satellite observations available across the geostationary

constellation (~1.7 x 4.5 km) as well as the most polluted metropolitan area in the TEMPO field of regard, making it an ideal location for TEMPO validation.

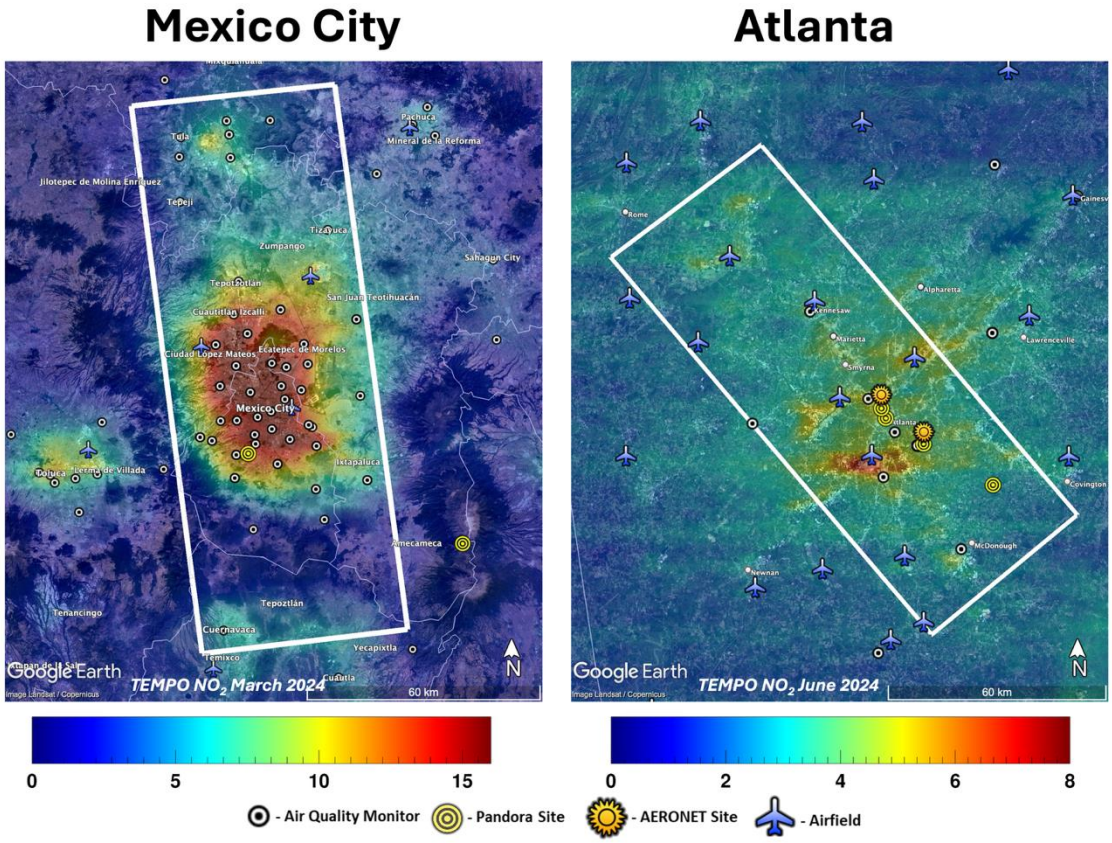

Figure 8. HAMAQ deployment locations showing average TEMPO NO_2 distribution (all hours) from candidate deployment months in each region, location of ground monitoring assets including Pandora and AERONET sites, and local airfields to be considered for missed approaches. The white box indicates the nominal sampling area for the B777.

Metro Atlanta provides a valuable perspective as a region hovering at the edge of compliance with the ozone and $PM_{2.5}$ National Ambient Air Quality Standards (NAAQS). From a satellite perspective, the area surrounding the world's busiest airport, Hartsfield-Jackson Atlanta International Airport dominates the emissions landscape of the region with respect to NO_2 (Figure 8). Metro Atlanta is also home to over 6 million residents making it 8th largest metropolitan area in the United States according to the US Census. Figure 9 shows how the ozone design value in Atlanta has fluctuated in recent years around the standard of 70 ppb. These design values, used to define NAAQS attainment status, are based on 4th highest 8-hour daily maximum ozone each year averaged over three years. The brief period with design values below 70 ppb is likely due to changes centered on the COVID-19 pandemic in 2020 [91]. While ozone exceedances in Atlanta can happen from spring through summer months, in the last five years, the month with the most predominant occurrence of ozone exceedances is June (total = 20 from 2021-2025) with at least 2 each year and a maximum of 7 (https://www.epa.gov/outdoor-air-quality-data/air-data-ozone-exceedances). This makes June the top contending month for the second HAMAQ deployment in 2028 despite the chance of mid-afternoon cumulus cloud fields obscuring the remote sensing point

of view (Figure 9). While having less seasonality, design values for the annual average of $PM_{2.5}$ in Metro Atlanta has decreased only slightly in the last decade from 10.5 to 9.4 $\mu g/m^3$, which meets the 2012 annual NAAQS of 12 $\mu g/m^3$ (https://www.epa.gov/air-trends/air-quality-design-values#map). However, in February 2024, the US EPA lowered this standard to 9 $\mu g/m^3$. The implementation of this standard is still under consideration but would put Atlanta into question for compliance with the new NAAQS.

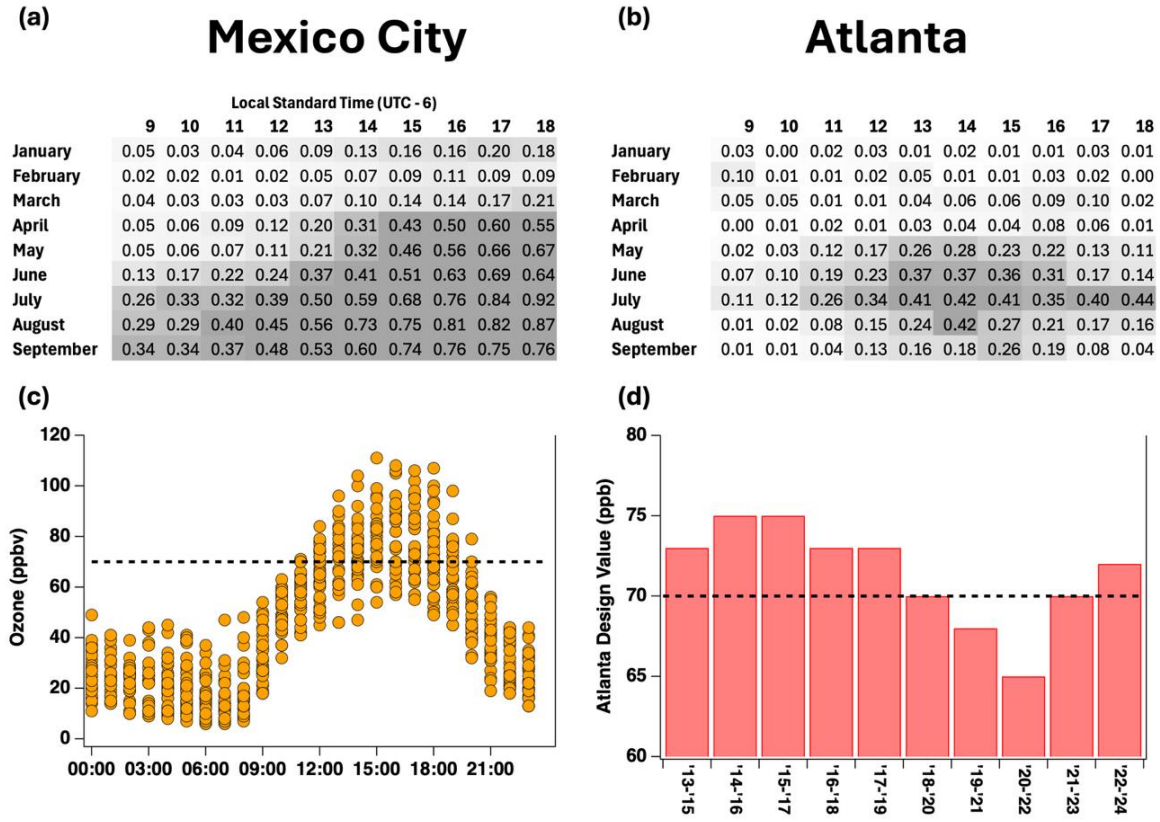

Mexico City	9	10	11	12	13	14	15	16	17	18
January	0.05	0.03	0.04	0.06	0.09	0.13	0.16	0.16	0.20	0.18
February	0.02	0.02	0.01	0.02	0.05	0.07	0.09	0.11	0.09	0.09
March	0.04	0.03	0.03	0.03	0.07	0.10	0.14	0.14	0.17	0.21
April	0.05	0.06	0.09	0.12	0.20	0.31	0.43	0.50	0.60	0.55
May	0.05	0.06	0.07	0.11	0.21	0.32	0.46	0.56	0.66	0.67
June	0.13	0.17	0.22	0.24	0.37	0.41	0.51	0.63	0.69	0.64
July	0.26	0.33	0.32	0.39	0.50	0.59	0.68	0.76	0.84	0.92
August	0.29	0.29	0.40	0.45	0.56	0.73	0.75	0.81	0.82	0.87
September	0.34	0.34	0.37	0.48	0.53	0.60	0.74	0.76	0.75	0.76

Atlanta	9	10	11	12	13	14	15	16	17	18
January	0.03	0.00	0.02	0.03	0.01	0.02	0.01	0.01	0.03	0.01
February	0.10	0.01	0.01	0.02	0.05	0.01	0.01	0.03	0.02	0.00
March	0.05	0.05	0.01	0.01	0.04	0.06	0.06	0.09	0.10	0.02
April	0.00	0.01	0.02	0.01	0.03	0.04	0.04	0.08	0.06	0.01
May	0.02	0.03	0.12	0.17	0.26	0.28	0.23	0.22	0.13	0.11
June	0.07	0.10	0.19	0.23	0.37	0.37	0.36	0.31	0.17	0.14
July	0.11	0.12	0.26	0.34	0.41	0.42	0.41	0.35	0.40	0.44
August	0.01	0.02	0.08	0.15	0.24	0.42	0.27	0.21	0.17	0.16
September	0.01	0.01	0.04	0.13	0.16	0.18	0.26	0.19	0.08	0.04

Figure 9. (a & b) Average cloud fractions from GOES-16 Clear Sky Mask each daytime hour from January-September (2020-2024) within a 1° box centered on Mexico City (a) and Atlanta (b). Whiter boxes indicate times when cloud fraction is quite low with the darkest grey representing a cloud fraction greater than 0.4, which is a typical threshold that impedes adequate satellite observations of air pollution. (c) Hourly ozone values at all Mexico City ground sites in March 2024 from https://www.aire.cdmx.gob.mx/default.php?opc=%27aKBhnmI=%27&opcion=Zg==.
(d) Maximum ozone design values in the Atlanta Core Based Statistical Area from 2015-present with the EPA National Ambient Air Quality Standard for ozone shown by the black dashed line from https://www.epa.gov/air-trends/air-quality-design-values.

An additional valuable contrast between the two locations relates to difference in their observed diurnal behavior for NO_2 and HCHO (Figure 10). For NO_2, Mexico City has a strong diurnal trend with a mid-morning peak and steep decline in the afternoon. Metro Atlanta shows no trend in the average, though is it expected that variability on individual days could be significant. For HCHO, both locations show an increase through the morning likely due to photochemical production. HCHO in Mexico City shows a downturn after peaking in the mid-afternoon, while HCHO in Metro Atlanta levels off at peak values through sunset. The strong contribution from biogenic

VOCs in Atlanta is likely responsible for the difference. Both validating and investigating the daily differences in these diurnal trends will help to understand the role of emissions, chemistry, and dynamics in determining daily air quality outcomes and the context that TEMPO can provide.

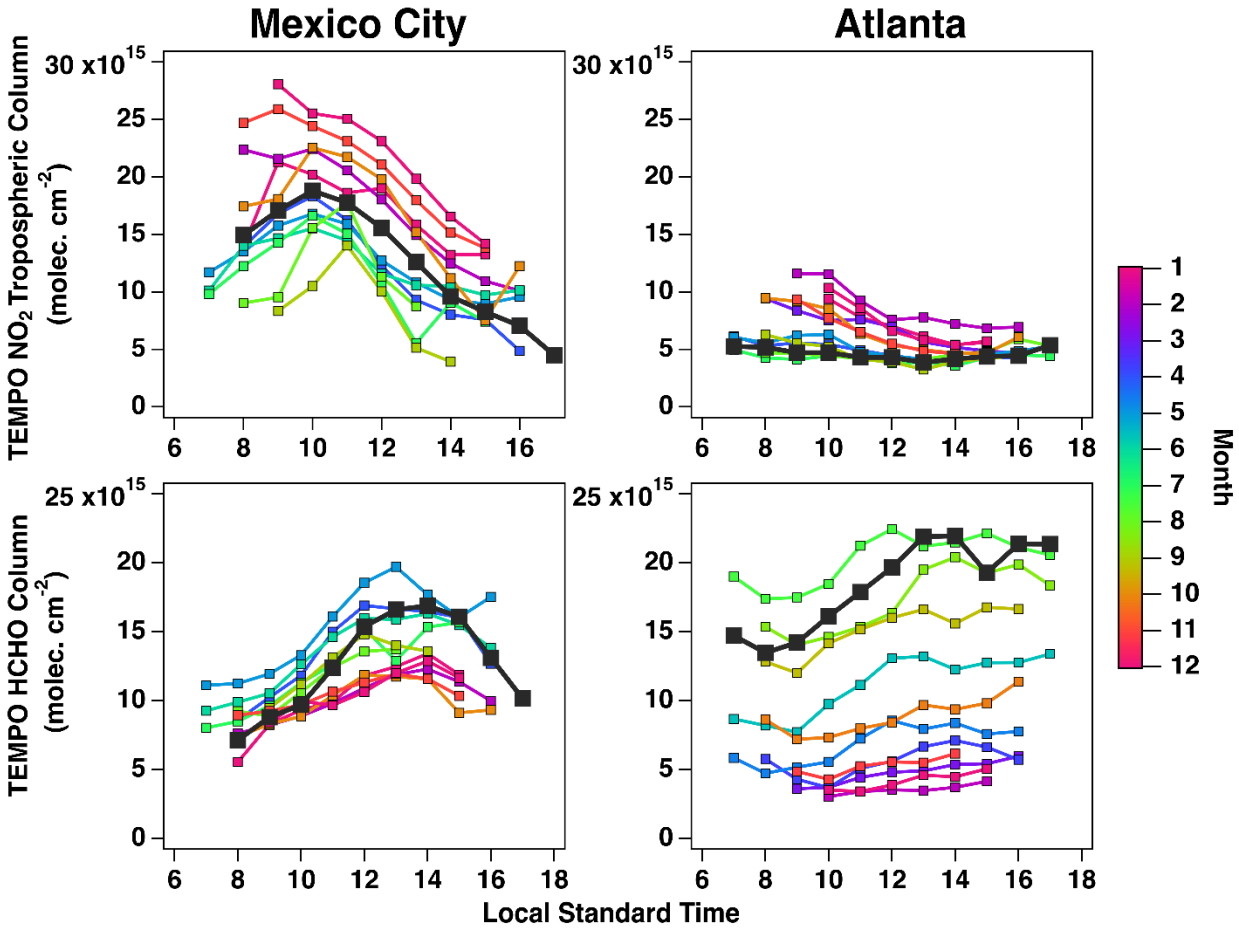

Figure 10. Monthly-average (colored) diurnal profiles of column tropospheric NO_2 (top) and HCHO (bottom) in Mexico City and Atlanta (averaged 20 km from the city center) from the TEMPO instrument. Data for candidate deployment months of March (Mexico City) and June (Atlanta) are shown in black.

The Role of Partners – The HAMAQ team will perform comprehensive measurements, modeling, and analysis by assembling a team based on the priorities outlined in the Appendix. However, it would be impossible to accomplish HAMAQ science objectives without collaboration with local partners.

For Mexico, collaborating partners include the Government of Mexico City, the Environmental Commission of the Megalopolis, the National University's Institute of Atmospheric Science and Climate Change, and the Mexican Space Agency. In Atlanta, collaboration is already underway with the TEMPO Science Team and the U.S. EPA, NSF, and Georgia EPD. It is expected that

collaboration with other federal, state and locally funded environmental agencies and organizations can grow in both regions.

The HAMAQ data is also expected to align with the interest of external research groups. The HAMAQ leadership team will encourage these and other groups to take advantage of the HAMAQ observations. HAMAQ will be of particular interest to two new IGAC initiatives, MAP-AQ (Monitoring, Analysis, and Prediction of Air Quality) and AMIGO (Analysis of eMIssions usinG Observations), in addition to the well-established GEIA (Global Emissions InitiAtive). HAMAQ will invite the leaders of these initiatives to science team meetings and send participants to their meetings as well.

Specific approaches to address each of the HAMAQ science objectives are discussed below.

Objective 1: Satellite-surface connections. Work on this objective will begin with pre-mission analysis in collaboration with local partners. Observations from surface networks, Pandora and AERONET sites, and satellite observations over each deployment location will be examined for diurnal patterns in column and surface abundances of trace gas and particulate pollution. Since these data sources provide long-term measurements, analysis will include seasonal trends for comparison with expectations during the deployment period. This will include basic comparisons between ground-based measurements and TEMPO to identify challenges within the retrievals relative to data interpretation as well as a priori inputs into satellite data products. Global and regional-scale model results will be compared to see if they reproduce the observed behaviors, and whether areas of model disagreement are co-located with discrepancies between satellites and ground-based remote sensing by Pandora and AERONET. Data assimilation will be conducted and assessed for improvements to model representation of surface-column behavior. After each deployment, these analyses will be extended to include comparisons of airborne *in situ* profiles with satellite a priori profiles and the various models to quantify the contribution of profile assumptions to uncertainties in remotely sensed column abundances both from the ground and satellites. This will include assessment of impacts due to vertical and horizontal gradients and other factors such as land surface characteristics, *a priori* profiles, clouds, and other meteorological conditions.

Objective 2: Emission Inventories. Work on this objective will begin with pre-mission model assimilation of satellite aerosol and trace gas retrievals to ensure that this capability will be operational during the deployments. This will include compilation of bottom-up inventories, both at global and regional scales, which are utilized as a-priori emissions in a data assimilation system and provide uncertainty estimation. Data assimilation methods will include emissions adjustment capability that can be operationalized in an air quality forecast during the field campaign. The differences between forecasts close and far from the assimilation time will be assessed to detect regions with significant deviations which can be an indicator of errors in emissions where deviations are persistent. Chemical tracer forecasts will also be employed to track both transport pathways and various regions with specific emissions sources. After each deployment, teams will evaluate how well models simulate *in situ* profiles of lower atmospheric composition and remotely sensed spatial and temporal variability in trace gases and aerosols. This will allow for identifying gaps in emission inventories motivating improvements through inverse modeling and model sensitivity studies. Assimilation of geostationary, along with polar-orbiting satellite observations will be performed to assess and improve emissions across the Northern Hemisphere, thus reducing

an additional error in simulations of the field area of interest. Detailed analysis of *in situ* observations will also be conducted to fingerprint sources and determine relative source contributions using established statistical methods (e.g., positive-matrix factorization).

Objective 3: Satellite proxies for air quality. Work on satellite proxies will begin with pre-mission analysis of observations from the Pandonia Global Network in collaboration with local partners. Data will be specifically analyzed to determine whether Pandora CH_2O columns and surface ozone exhibit predictable behavior either consistently or intermittently and under what meteorological and/or chemical conditions. Additional examination of Pandora observations of CH_2O:NO_2 will be conducted to assess the diurnal variability in this quantity and whether it exhibits different behavior during air quality episodes. Complementing these analyses, pre-mission air quality simulations over the deployment regions will be used to evaluate these relationships in the model world and determine differences worthy of investigation. Where these proxies show utility, satellite observations will be evaluated for the regional perspective and how it might influence the deployment sampling strategy for the remote sensing aircraft. After each deployment, remote sensing observations from the B777 will enable a much broader assessment of these proxies and the conditions that enable or limit their use. Detailed airborne *in situ* data on aerosol composition, CH_2O, NO_2, and SO_2 during the deployments will also support further development of satellite proxies for secondary OA. Results of these analyses will help models to more effectively extrapolate the degree to which these proxies can be expected to provide useful information. To this end, global and regional model output will be combined with ground and satellite measurements to conduct a comprehensive analysis of the correlation between column abundances of CH_2O, NO_2, SO_2, and AOD with surface ozone and $PM_{2.5}$ across the entire Northern Hemisphere, aiming to form a systematic understanding of the behavior, applicability, and limitations of these satellite proxies at various spatial and temporal scales. These results ultimately determine the utility of these proxies for future satellite observations in air quality management.

Objective 4: Diversity in Factors Controlling Air Quality. This objective will be supported by global to regional simulations from the modeling groups for post-mission analysis. The comprehensive suite of trace gas and aerosol model outputs will be evaluated with the HAMAQ coordinated ground, aircraft, and satellite observations to identify model strengths and weaknesses. The use of tagged tracers from a variety of sources, including global and regional emissions from anthropogenic, biomass burning and natural (dust, biogenic) sources for aerosols and trace gases (CO, NO_2, etc.) will provide the perspectives needed to assess local versus transboundary influences. A diversity in controlling factors of air quality between the two regions is expected. Interpretation of observations with models will be used to understand the relative importance of regional pollution sources, transboundary transport, and meteorological parameters (e.g., boundary layer height, humidity, winds, and precipitation) will aid in identifying the key factors controlling O_3 and aerosol abundances in different locations and times. Box model simulations will provide observationally constrained budgets of ozone production and predictions of radical budgets that drive photochemistry. Model output from different systems will be compared with each other and against observations for a full evaluation and identification of multi-model deficiencies, such as representation of chemistry, transport, or other physical processes (e.g., deposition) and to examine common limitations in satellite retrievals. There is a growing understanding that urban characteristics, such as the heat island effect, impact pollutant levels (e.g., [88]). Initial post-campaign analysis will correlate surface temperature (measured from the aircraft) with boundary layer height to determine whether this model characteristic (e.g., urban heat) helps to capture these variations.

Opportunities for Cross-Disciplinary Science

The relationship between meteorology and chemistry is well recognized, but a more balanced approach to exploring their interaction in field observations is still needed [89]. Using the NASA B777 for remote sensing opens the door to a dramatic expansion in observations that could enable a deeper exploration of the connections between air quality, planetary boundary layer dynamics, land surface impacts, greenhouse gas emissions, etc. During KORUS-AQ, changes in fine particle pollution were linked to a combination of long-range transport, greater containment due to shallow boundary layer mixing, increased gas-to-particle conversion under humid conditions, and deepening of the nocturnal boundary layer [27, 84]. Despite evidence of these impacts, their quantification and representation in models remains difficult. Additional early, yet-unpublished results from ASIA-AQ show that model treatment of boundary layer conditions over China has a large influence on the amount of pollution that is transported downwind versus remains in the source region. The largest differences relate to the timing of the afternoon breakdown in mixing as well as the depth of the nocturnal boundary layer. These are the times of day when observing boundary layer mixing is most difficult. To complement the planned HAMAQ observations of trace gas columns and profiles of aerosol and ozone, guest observations of water vapor profiles and 3-D winds would provide the most value for constraining models. As this would not exhaust the capacity for hosted instruments, observations of land-surface characteristics, soil moisture, and greenhouse gases (e.g., shortwave infrared) and other reactive gases (e.g., thermal infrared) would provide an unprecedented level of detail for understanding and improving predictability for how urban regions impact atmospheric composition and dynamics both locally and downwind.

Appendix of Measurement and Model Requirements

Table 1. Science Measurement Requirement Matrix (P=priority, v.=vertical, h.=horizontal (x,y), a.t.=along track)

Remote Sensing Aircraft	**P[1]**	**Uncertainty[2]**	**Resolution[3]**	**SQs**
Column densities:				
Nitrogen Dioxide (NO_2)	1	$1x10^{15}$ molec. cm^{-2} (slant column)	h. 500 m	1,2,3,4
Formaldehyde (CH_2O)	1	$1x10^{16}$ molec. cm^{-2} (slant column)	h. 500 m	1,2,3,4
Sulfur Dioxide (SO_2)	2	$4x10^{15}$ molec. cm^{-2} (slant column)	h. 500 m	1,2,3,4
Glyoxal (CHOCHO)	3	$5x10^{14}$ molec. cm^{-2} (slant column)	h. 500 m	1,2,3,4
Profiles:				
Aerosol backscatter	1	0.2 Mm^{-1} sr^{-1}	v. 30 m, a.t. 2 km	1,2,4
Aerosol extinction	1	0.01 km^{-1}	v. 300 m, a.t. 12 km	1,2,4
Aerosol depolarization	1	1%	v. 30 m, a.t. 2 m	1,2,4
Ozone (O_3)	1	5 ppb or 15%	v. 300 m, a.t. 12 km	1,2,3,4
Surface variables:				
Surface Temperature Gradient	2	<1 C	a.t. 400 m	1,2,4
***In situ* Aircraft**	**P[1]**	**Uncertainty[2]**	**Time Resolution**	**SQs**
Trace Gases:				
Ozone (O_3)	1	5 ppb or 10%	1 s	1,2,3,4
Nitric Oxide (NO)	1	30 ppt or 20%	1 s	2,4
Nitrogen Dioxide (NO_2)	1	50 ppt or 30%	1 s	1,2,3,4
Formaldehyde (CH_2O)	1	60 ppt or 10%	1 s	1,2,3,4
Water Vapor (H_2Ov)	1	5%	1 s	1,4
Carbon Monoxide (CO)	1	2 ppb or 2%	1 s	2,4
Carbon Dioxide (CO_2)	1	0.25 ppm	1 s	2,4
Methane (CH_4)	1	1%	1 s	2,4
Speciated hydrocarbons[4]	1	variable (1-10 ppt or 10%)	variable (s to min)	2,4
Ethane (C_2H_6)	2	50 ppt or 5%	1 s	2,4
Sulfur Dioxide (SO_2)	2	20 ppt or 30%	1 s	1,2,3,4
Total Reactive Nitrogen (NOy)	2	100 ppt or 30%	1 s	2,4
Speciated reactive nitrogen[5]	2	variable (10-30%)	1 s	2,4
Tracer compounds[6]	2	variable (1-10 ppt or 10%)	variable (s to min)	2,4
Ammonia (NH_3)	2	20%	1 s	2,4
Nitrous Oxide (N_2O)	3	1%	1 s	2,4
Peroxides (H_2O_2 and ROOH)	3	50 ppt or 30%	1 s	2,4
Glyoxal (CHOCHO)	3	50 ppt or 10%	1 s	2,3,4
Aerosols:				
Number	1	10%	1 s	2,4
Size Distribution (10 nm - 5 µm)	1	20%	1 s	2,4
Scattering (multi-wavelength)	1	0.5 Mm^{-1}	1 s	2,4
Absorption (multi-wavelength)	1	0.5 Mm^{-1}	1 s	2,4
Hygroscopicity, f(RH)	1	20%	1 s	2,4
Nonrefractory mass composition	1	35%	1 s	2,3,4
Black Carbon mass	1	20%	1 s	2,4
BrC absorption	2	20%	1 s	2,4
Radiation and Met:				
Spectral Actinic Flux (4π sr)	1	10%	3 s	4
Met (T, P, RH, 2-D winds)	1	0.3 K, 0.3 mb, 15%, 1 m/s	1 s	1,2,4

[1]Priority 1 measurements are considered Threshold, while all measurements are included in the Baseline requirements.

[2]When stated as a mixing ratio "or" percent, uncertainty is the greater of the two values. Many of these values are taken directly from archived data from recent airborne field campaigns.

[3]Along track resolutions for profile data improve significantly when products are averaged over the boundary layer depth.

[4]Depending on the technique(s) selected, there are tradeoffs between time resolution and number of compounds detected. Speciated hydrocarbons can include C_2-C_{10} alkanes, C_2-C_4 alkenes, C_6-C_9 aromatics, C_1-C_5 alkylnitrates, C_1-C_2 halocarbons, isoprene, monoterpenes, 1,3-butadiene, oxygenated hydrocarbons, etc.

[5]Depending on the technique(s) selected, speciated reactive nitrogen can include Nitric Acid (HNO_3), Nitrous Acid (HONO), Peroxyacetylnitrate compounds (PANs), Alkylnitrate compounds (ANs), Nitrylchloride ($ClNO_2$), etc.

[6]Depending on the technique(s) selected, there are tradeoffs between time resolution and number of compounds detected. Tracers include Hydrogen Cyanide (HCN), Acetonitrile (CH_3CN), Carbonyl sulfide (OCS), speciated halocarbons, etc.

Table 2. Science Modeling Requirement Matrix (P=priority, v.=vertical, h.=horizontal (x,y))

Scientific Modeling Capability	P[1]	Modeling Requirements	SQs
Global model	1	h. 0.25 deg, v. 60m in the boundary layer; with ability to nest targeted domains, implement tagged tracers, provide 5-day hourly forecasting, real time visualization and comparison with observations	1,2,3,4
Regional model	1	h. 4 km, v. 30m in the boundary layer; with ability to nest targeted domains, implement tagged tracers, provide 2-day hourly forecasting, real time visualization and comparison with observations	1,2,3,4
0-D photochemical box model	2	Photochemical modeling based on in situ observed quantities with choice of mechanism (e.g., MCM, SAPRC, RADM, etc.)	3,4

[1]Priority 1 models are considered Threshold, while all models contribute to the Baseline requirements.

References

[1] CEOS, "White Paper: Geostationary Satellite Constellation for Observing Global Air Quality: Geophysical Validation Needs," Committee on Earth Observation Satellites, 2019. Accessed: Apr. 18, 2023. [Online]. Available: https://ceos.org/document_management/Virtual_Constellations/ACC/Documents/GEO%20AQ%20Constellation%20Geophysical%20Validation%20Needs%201.1%202Oct2019.pdf

[2] P. J. Landrigan *et al.*, "The Lancet Commission on pollution and health," *The Lancet*, vol. 391, no. 10119, pp. 462–512, Feb. 2018, https://doi.org/10.1016/S0140-6736(17)32345-0

[3] Q. Di *et al.*, "Air Pollution and Mortality in the Medicare Population," *N Engl J Med*, vol. 376, no. 26, pp. 2513–2522, Jun. 2017, https://doi.org/10.1056/NEJMoa1702747

[4] OECD, *The Economic Consequences of Outdoor Air Pollution*. OECD, 2016. https://doi.org/10.1787/9789264257474-en

[5] R. Van Dingenen, F. J. Dentener, F. Raes, M. C. Krol, L. Emberson, and J. Cofala, "The global impact of ozone on agricultural crop yields under current and future air quality legislation," *Atmospheric Environment*, vol. 43, no. 3, pp. 604–618, Jan. 2009, https://doi.org/10.1016/j.atmosenv.2008.10.033

[6] Z. Feng *et al.*, "Ozone pollution threatens the production of major staple crops in East Asia," *Nat Food*, vol. 3, no. 1, pp. 47–56, Jan. 2022, https://doi.org/10.1038/s43016-021-00422-6

[7] J. Kim *et al.*, "New Era of Air Quality Monitoring from Space: Geostationary Environment Monitoring Spectrometer (GEMS)," *Bulletin of the American Meteorological Society*, vol. 101, no. 1, pp. E1–E22, Jan. 2020, https://doi.org/10.1175/BAMS-D-18-0013.1

[8] P. Zoogman *et al.*, "Tropospheric emissions: Monitoring of pollution (TEMPO)," *Journal of Quantitative Spectroscopy and Radiative Transfer*, vol. 186, pp. 17–39, Jan. 2017, https://doi.org/10.1016/j.jqsrt.2016.05.008

[9] M. G. Kolm *et al.*, "Sentinel 4: a geostationary imaging UVN spectrometer for air quality monitoring: status of design, performance and development," in *International Conference on Space Optics — ICSO 2014*, B. Cugny, Z. Sodnik, and N. Karafolas, Eds., Tenerife, Canary Islands, Spain: SPIE, Nov. 2017, p. 39. https://doi.org/10.1117/12.2304099

[10] J. P. Veefkind *et al.*, "TROPOMI on the ESA Sentinel-5 Precursor: A GMES mission for global observations of the atmospheric composition for climate, air quality and ozone layer applications," *Remote Sensing of Environment*, vol. 120, pp. 70–83, May 2012, https://doi.org/10.1016/j.rse.2011.09.027

[11] DISCOVER-AQ Science Team, "DISCOVER-AQ Campaign." NASA Langley Atmospheric Science Data Center DAAC, 2014. https://doi.org/10.5067/AIRCRAFT/DISCOVER-AQ/AEROSOL-TRACEGAS

[12] G. Chen, "KORUS-AQ Airborne Mission Overview," https://doi.org/10.5067/SUBORBITAL/KORUSAQ/DATA01

[13] LISTOS Science Team, "Long Island Sound Tropospheric Ozone Study." NASA Langley Atmospheric Science Data Center DAAC, 2020. https://doi.org/10.5067/SUBORBITAL/LISTOS/DATA001

[14] TRACER-AQ Science Team, "TRACER-AQ – TRacking Aerosol Convection ExpeRiment - Air Quality." Accessed: Apr. 18, 2023. [Online]. Available: https://www-air.larc.nasa.gov/missions/tracer-aq/index.html

[15] ASIA-AQ Science Team, "Airborne and Satellite Investigation of Asian Air Quality." Accessed: Apr. 18, 2023. [Online]. Available: https://espo.nasa.gov/asia-aq/content/ASIA-AQ
[16] NOAA Chemical Sciences Lab, "AGES+." Accessed: Apr. 18, 2023. [Online]. Available: https://csl.noaa.gov/projects/ages/
[17] L. N. Lamsal *et al.*, "High-resolution NO_2 observations from the Airborne Compact Atmospheric Mapper: Retrieval and validation," *Journal of Geophysical Research: Atmospheres*, vol. 122, no. 3, pp. 1953–1970, 2017, https://doi.org/10.1002/2016JD025483
[18] J.-T. Lin *et al.*, "Retrieving tropospheric nitrogen dioxide from the Ozone Monitoring Instrument: effects of aerosols, surface reflectance anisotropy, and vertical profile of nitrogen dioxide," *Atmos. Chem. Phys.*, vol. 14, no. 3, pp. 1441–1461, Feb. 2014, https://doi.org/10.5194/acp-14-1441-2014
[19] A. Lorente *et al.*, "Structural uncertainty in air mass factor calculation for NO_2 and HCHO satellite retrievals," *Atmos. Meas. Tech.*, vol. 10, no. 3, pp. 759–782, Mar. 2017, https://doi.org/10.5194/amt-10-759-2017
[20] L. M. Judd *et al.*, "Evaluating Sentinel-5P TROPOMI tropospheric NO_2 column densities with airborne and Pandora spectrometers near New York City and Long Island Sound," *Atmos. Meas. Tech.*, vol. 13, no. 11, pp. 6113–6140, Nov. 2020, https://doi.org/10.5194/amt-13-6113-2020
[21] J. H. Crawford *et al.*, "Multi-perspective Observations of Nitrogen Dioxide over Denver during DISCOVER-AQ: Insights for Future Monitoring," *EM Magazine*, Aug. 2016. Accessed: Apr. 19, 2023. [Online]. Available: https://airandwmapa.sharepoint.com/sites/AWMA_Website/Shared%20Documents/Forms/AllItems.aspx?id=%2Fsites%2FAWMA%5FWebsite%2FShared%20Documents%2Fem%2Ddo%20not%20delete%2F2016%2F8%2Fcrawford%2Epdf&parent=%2Fsites%2FAWMA%5FWebsite%2FShared%20Documents%2Fem%2Ddo%20not%20delete%2F2016%2F8&p=true&ga=1
[22] J. H. Crawford *et al.*, "The Korea–United States Air Quality (KORUS-AQ) field study," *Elementa: Science of the Anthropocene*, vol. 9, no. 1, p. 00163, May 2021, https://doi.org/10.1525/elementa.2020.00163
[23] S. Crumeyrolle *et al.*, "Factors that influence surface PM_{2.5} values inferred from satellite observations: perspective gained for the US Baltimore–Washington metropolitan area during DISCOVER-AQ," *Atmos. Chem. Phys.*, vol. 14, no. 4, pp. 2139–2153, Feb. 2014, https://doi.org/10.5194/acp-14-2139-2014
[24] A. J. Beyersdorf *et al.*, "The impacts of aerosol loading, composition, and water uptake on aerosol extinction variability in the Baltimore–Washington, D.C. region," *Atmos. Chem. Phys.*, vol. 16, no. 2, pp. 1003–1015, Jan. 2016, https://doi.org/10.5194/acp-16-1003-2016
[25] L. D. Ziemba *et al.*, "Airborne observations of aerosol extinction by in situ and remote-sensing techniques: Evaluation of particle hygroscopicity," *Geophys. Res. Lett.*, vol. 40, no. 2, pp. 417–422, Jan. 2013, https://doi.org/10.1029/2012GL054428
[26] Y. J. Oak *et al.*, "Evaluation of simulated O3 production efficiency during the KORUS-AQ campaign: Implications for anthropogenic NOx emissions in Korea," *Elem Sci Anth*, vol. 7, no. 1, p. 56, Dec. 2019, https://doi.org/10.1525/elementa.394
[27] C. Jordan *et al.*, "Investigation of factors controlling $PM_{2.5}$ variability across the South Korean Peninsula during KORUS-AQ," *Elem Sci Anth*, vol. 8, no. 1, p. 28, Jul. 2020, https://doi.org/10.1525/elementa.424

[28] D. L. Goldberg *et al.*, "CAMx ozone source attribution in the eastern United States using guidance from observations during DISCOVER-AQ Maryland," *Geophys. Res. Lett.*, vol. 43, no. 5, pp. 2249–2258, Mar. 2016, https://doi.org/10.1002/2015GL067332

[29] H. Chong *et al.*, "High-resolution mapping of SO_2 using airborne observations from the GeoTASO instrument during the KORUS-AQ field study: PCA-based vertical column retrievals," *Remote Sensing of Environment*, vol. 241, p. 111725, May 2020, https://doi.org/10.1016/j.rse.2020.111725

[30] J. Choi *et al.*, "An Inversion Framework for Optimizing Non-Methane VOC Emissions Using Remote Sensing and Airborne Observations in Northeast Asia During the KORUS-AQ Field Campaign," *JGR Atmospheres*, vol. 127, no. 7, Apr. 2022, https://doi.org/10.1029/2021JD035844

[31] H.-A. Kwon *et al.*, "Top-down estimates of anthropogenic VOC emissions in South Korea using formaldehyde vertical column densities from aircraft during the KORUS-AQ campaign," *Elementa: Science of the Anthropocene*, vol. 9, no. 1, p. 00109, Apr. 2021, https://doi.org/10.1525/elementa.2021.00109

[32] E. von Schneidemesser *et al.*, "Comparing Urban Anthropogenic NMVOC Measurements with Representation in Emission Inventories - A Global Perspective," *JGR Atmospheres*, p. e2022JD037906, Apr. 2023, https://doi.org/10.1029/2022JD037906

[33] M. Bauwens, B. Verreyken, T. Stavrakou, J.-F. Müller, and I. D. Smedt, "Spaceborne evidence for significant anthropogenic VOC trends in Asian cities over 2005–2019," *Environ. Res. Lett.*, vol. 17, no. 1, p. 015008, Jan. 2022, https://doi.org/10.1088/1748-9326/ac46eb

[34] L. C. Valin, A. M. Fiore, K. Chance, and G. González Abad, "The role of OH production in interpreting the variability of CH $_2$ O columns in the southeast U.S.: OH, VOC and CH $_2$ O Columns in the SOUTHEAST U.S.A.," *J. Geophys. Res. Atmos.*, vol. 121, no. 1, pp. 478–493, Jan. 2016, https://doi.org/10.1002/2015JD024012

[35] V. Natraj *et al.*, "Multi-spectral sensitivity studies for the retrieval of tropospheric and lowermost tropospheric ozone from simulated clear-sky GEO-CAPE measurements," *Atmospheric Environment*, vol. 45, no. 39, pp. 7151–7165, Dec. 2011, https://doi.org/10.1016/j.atmosenv.2011.09.014

[36] E. Hache *et al.*, "The added value of a visible channel to a geostationary thermal infrared instrument to monitor ozone for air quality," *Atmos. Meas. Tech.*, vol. 7, no. 7, pp. 2185–2201, Jul. 2014, https://doi.org/10.5194/amt-7-2185-2014

[37] T. O. Sato *et al.*, "Vertical profile of tropospheric ozone derived from synergetic retrieval using three different wavelength ranges, UV, IR, and microwave: sensitivity study for satellite observation," *Atmos. Meas. Tech.*, vol. 11, no. 3, pp. 1653–1668, Mar. 2018, https://doi.org/10.5194/amt-11-1653-2018

[38] J. R. Schroeder *et al.*, "Formaldehyde column density measurements as a suitable pathway to estimate near-surface ozone tendencies from space," *J. Geophys. Res. Atmos.*, vol. 121, no. 21, p. 13,088-13,112, Nov. 2016, https://doi.org/10.1002/2016JD025419

[39] K. R. Travis *et al.*, "Can Column Formaldehyde Observations Inform Air Quality Monitoring Strategies for Ozone and Related Photochemical Oxidants?," *JGR Atmospheres*, vol. 127, no. 13, Jul. 2022, https://doi.org/10.1029/2022JD036638

[40] D. L. Goldberg *et al.*, "Urban NO $_x$ emissions around the world declined faster than anticipated between 2005 and 2019," *Environ. Res. Lett.*, vol. 16, no. 11, p. 115004, Nov. 2021, https://doi.org/10.1088/1748-9326/ac2c34

[41] L. Zhu *et al.*, "Long-term (2005-2014) trends in formaldehyde (HCHO) columns across North America as seen by the OMI satellite instrument: Evidence of changing emissions of volatile organic compounds: HCHO Trend Across North America," *Geophys. Res. Lett.*, vol. 44, no. 13, pp. 7079–7086, Jul. 2017, https://doi.org/10.1002/2017GL073859

[42] E. Spinei *et al.*, "Effect of polyoxymethylene (POM-H Delrin) off-gassing within the Pandora head sensor on direct-sun and multi-axis formaldehyde column measurements in 2016–2019," *Atmos. Meas. Tech.*, vol. 14, no. 1, pp. 647–663, Jan. 2021, https://doi.org/10.5194/amt-14-647-2021

[43] M. A. G. Demetillo *et al.*, "Observing Nitrogen Dioxide Air Pollution Inequality Using High-Spatial-Resolution Remote Sensing Measurements in Houston, Texas," *Environ. Sci. Technol.*, vol. 54, no. 16, pp. 9882–9895, Aug. 2020, https://doi.org/10.1021/acs.est.0c01864

[44] I. M. Dressel *et al.*, "Daily Satellite Observations of Nitrogen Dioxide Air Pollution Inequality in New York City, New York and Newark, New Jersey: Evaluation and Application," *Environ. Sci. Technol.*, vol. 56, no. 22, pp. 15298–15311, Nov. 2022, https://doi.org/10.1021/acs.est.2c02828

[45] E. A. Marais *et al.*, "Aqueous-phase mechanism for secondary organic aerosol formation from isoprene: application to the southeast United States and co-benefit of SO2 emission controls," *Atmos. Chem. Phys.*, vol. 16, no. 3, pp. 1603–1618, Feb. 2016, https://doi.org/10.5194/acp-16-1603-2016

[46] J. Liao *et al.*, "Towards a satellite formaldehyde – in situ hybrid estimate for organic aerosol abundance," *Atmos. Chem. Phys.*, vol. 19, no. 5, pp. 2765–2785, Mar. 2019, https://doi.org/10.5194/acp-19-2765-2019

[47] Q. Zhang *et al.*, "Ubiquity and dominance of oxygenated species in organic aerosols in anthropogenically-influenced Northern Hemisphere midlatitudes," *Geophys. Res. Lett.*, vol. 34, no. 13, p. n/a-n/a, Jul. 2007, https://doi.org/10.1029/2007GL029979

[48] R. V. Martin *et al.*, "Evaluation of GOME satellite measurements of tropospheric NO2 and HCHO using regional data from aircraft campaigns in the southeastern United States," *J. Geophys. Res.*, vol. 109, no. D24, p. D24307, Dec. 2004, https://doi.org/10.1029/2004JD004869

[49] B. N. Duncan *et al.*, "Application of OMI observations to a space-based indicator of NOx and VOC controls on surface ozone formation," *Atmospheric Environment*, vol. 44, no. 18, pp. 2213–2223, Jun. 2010, https://doi.org/10.1016/j.atmosenv.2010.03.010

[50] J. C. Witte, B. N. Duncan, A. R. Douglass, T. P. Kurosu, K. Chance, and C. Retscher, "The unique OMI HCHO/NO_2 feature during the 2008 Beijing Olympics: Implications for ozone production sensitivity," *Atmospheric Environment*, vol. 45, no. 18, pp. 3103–3111, Jun. 2011, https://doi.org/10.1016/j.atmosenv.2011.03.015

[51] E. A. Marais *et al.*, "Anthropogenic emissions in Nigeria and implications for atmospheric ozone pollution: A view from space," *Atmospheric Environment*, vol. 99, pp. 32–40, Dec. 2014, https://doi.org/10.1016/j.atmosenv.2014.09.055

[52] X. Jin and T. Holloway, "Spatial and temporal variability of ozone sensitivity over China observed from the Ozone Monitoring Instrument," *J. Geophys. Res. Atmos.*, vol. 120, no. 14, p. 2015JD023250, Jul. 2015, https://doi.org/10.1002/2015JD023250

[53] A. S. Mahajan *et al.*, "Inter-annual variations in satellite observations of nitrogen dioxide and formaldehyde over India," *Atmospheric Environment*, vol. 116, pp. 194–201, Sep. 2015, https://doi.org/10.1016/j.atmosenv.2015.06.004

[54] G. Tang, Y. Wang, X. Li, D. Ji, S. Hsu, and X. Gao, "Spatial-temporal variations in surface ozone in Northern China as observed during 2009–2010 and possible implications for future air quality control strategies," *Atmos. Chem. Phys.*, vol. 12, no. 5, pp. 2757–2776, Mar. 2012, https://doi.org/10.5194/acp-12-2757-2012

[55] Y. Choi, H. Kim, D. Tong, and P. Lee, "Summertime weekly cycles of observed and modeled NOx and O_3 concentrations as a function of satellite-derived ozone production sensitivity and land use types over the Continental United States," *Atmos. Chem. Phys.*, vol. 12, no. 14, pp. 6291–6307, Jul. 2012, https://doi.org/10.5194/acp-12-6291-2012

[56] J. R. Schroeder *et al.*, "New insights into the column CH_2O/NO_2 ratio as an indicator of near-surface ozone sensitivity," *J. Geophys. Res. Atmos.*, vol. 122, no. 16, p. 2017JD026781, Aug. 2017, https://doi.org/10.1002/2017JD026781

[57] A. H. Souri *et al.*, "Characterization of errors in satellite-based $HCHO/NO_2$ tropospheric column ratios with respect to chemistry, column-to-PBL translation, spatial representation, and retrieval uncertainties," *Atmos. Chem. Phys.*, vol. 23, no. 3, pp. 1963–1986, Feb. 2023, https://doi.org/10.5194/acp-23-1963-2023

[58] F. Wittrock *et al.*, "Simultaneous global observations of glyoxal and formaldehyde from space," *Geophys. Res. Lett.*, vol. 33, no. 16, p. L16804, 2006, https://doi.org/10.1029/2006GL026310

[59] L. M. A. Alvarado *et al.*, "Unexpected long-range transport of glyoxal and formaldehyde observed from the Copernicus Sentinel-5 Precursor satellite during the 2018 Canadian wildfires," *Atmos. Chem. Phys.*, vol. 20, no. 4, pp. 2057–2072, Feb. 2020, https://doi.org/10.5194/acp-20-2057-2020

[60] C. Lerot, J. -F. Müller, N. Theys, I. De Smedt, T. Stavrakou, and M. Van Roozendael, "Satellite Evidence for Glyoxal Depletion in Elevated Fire Plumes," *Geophysical Research Letters*, vol. 50, no. 4, Feb. 2023, https://doi.org/10.1029/2022GL102195

[61] C. Chan Miller *et al.*, "Glyoxal yield from isoprene oxidation and relation to formaldehyde: chemical mechanism, constraints from SENEX aircraft observations, and interpretation of OMI satellite data," *Atmos. Chem. Phys.*, vol. 17, no. 14, pp. 8725–8738, Jul. 2017, https://doi.org/10.5194/acp-17-8725-2017

[62] J. P. DiGangi *et al.*, "Observations of glyoxal and formaldehyde as metrics for the anthropogenic impact on rural photochemistry," *Atmos. Chem. Phys.*, vol. 12, no. 20, pp. 9529–9543, Oct. 2012, https://doi.org/10.5194/acp-12-9529-2012

[63] J. Kaiser *et al.*, "Reassessing the ratio of glyoxal to formaldehyde as an indicator of hydrocarbon precursor speciation," *Atmos. Chem. Phys.*, vol. 15, no. 13, pp. 7571–7583, Jul. 2015, https://doi.org/10.5194/acp-15-7571-2015

[64] C. Lerot *et al.*, "Glyoxal tropospheric column retrievals from TROPOMI – multi-satellite intercomparison and ground-based validation," *Atmos. Meas. Tech.*, vol. 14, no. 12, pp. 7775–7807, Dec. 2021, https://doi.org/10.5194/amt-14-7775-2021

[65] G. M. Mazzuca *et al.*, "Ozone production and its sensitivity to NOx and VOCs: results from the DISCOVER-AQ field experiment, Houston 2013," *Atmos. Chem. Phys.*, vol. 16, no. 22, pp. 14463–14474, Nov. 2016, https://doi.org/10.5194/acp-16-14463-2016.

[66] S. Pan, Y. Choi, A. Roy, X. Li, W. Jeon, and A. H. Souri, "Modeling the uncertainty of several VOC and its impact on simulated VOC and ozone in Houston, Texas," *Atmospheric Environment*, vol. 120, pp. 404–416, Nov. 2015, https://doi.org/10.1016/j.atmosenv.2015.09.029

[67] M. S. Johnson *et al.*, "Analyzing source apportioned methane in northern California during Discover-AQ-CA using airborne measurements and model simulations," *Atmospheric Environment*, vol. 99, pp. 248–256, Dec. 2014, https://doi.org/10.1016/j.atmosenv.2014.09.068
[68] A. Townsend-Small *et al.*, "Using stable isotopes of hydrogen to quantify biogenic and thermogenic atmospheric methane sources: A case study from the Colorado Front Range," *Geophys. Res. Lett.*, vol. 43, no. 21, Nov. 2016, https://doi.org/10.1002/2016GL071438
[69] H. S. Halliday *et al.*, "Atmospheric benzene observations from oil and gas production in the Denver-Julesburg Basin in July and August 2014," *JGR Atmospheres*, vol. 121, no. 18, Sep. 2016, https://doi.org/10.1002/2016JD025327
[70] L. C. Cheadle *et al.*, "Surface ozone in the Colorado northern Front Range and the influence of oil and gas development during FRAPPE/DISCOVER-AQ in summer 2014," *Elementa: Science of the Anthropocene*, vol. 5, p. 61, Jan. 2017, https://doi.org/10.1525/elementa.254
[71] C. P. Loughner *et al.*, "Impact of Bay-Breeze Circulations on Surface Air Quality and Boundary Layer Export," *Journal of Applied Meteorology and Climatology*, vol. 53, no. 7, pp. 1697–1713, Jul. 2014, https://doi.org/10.1175/JAMC-D-13-0323.1
[72] R. M. Stauffer *et al.*, "Bay breeze influence on surface ozone at Edgewood, MD during July 2011," *J Atmos Chem*, vol. 72, no. 3–4, pp. 335–353, Sep. 2015, https://doi.org/10.1007/s10874-012-9241-6
[73] J. T. Sullivan *et al.*, "Quantifying the contribution of thermally driven recirculation to a high-ozone event along the Colorado Front Range using lidar," *J. Geophys. Res. Atmos.*, vol. 121, no. 17, p. 10,377-10,390, Sep. 2016, https://doi.org/10.1002/2016JD025229
[74] K. T. Vu *et al.*, "Impacts of the Denver Cyclone on regional air quality and aerosol formation in the Colorado Front Range during FRAPPÉ 2014," *Atmos. Chem. Phys.*, vol. 16, no. 18, pp. 12039–12058, Sep. 2016, https://doi.org/10.5194/acp-16-12039-2016
[75] B. C. McDonald *et al.*, "Volatile chemical products emerging as largest petrochemical source of urban organic emissions," *Science*, vol. 359, no. 6377, pp. 760–764, Feb. 2018, https://doi.org/10.1126/science.aaq0524
[76] I. J. Simpson *et al.*, "Characterization, sources and reactivity of volatile organic compounds (VOCs) in Seoul and surrounding regions during KORUS-AQ," *Elementa: Science of the Anthropocene*, vol. 8, p. 37, Jan. 2020, https://doi.org/10.1525/elementa.434
[77] Y. Peng, A. P. Mouat, Y. Hu, M. Li, B. C. McDonald, and J. Kaiser, "Source appointment of volatile organic compounds and evaluation of anthropogenic monoterpene emission estimates in Atlanta, Georgia," *Atmospheric Environment*, vol. 288, p. 119324, Nov. 2022, https://doi.org/10.1016/j.atmosenv.2022.119324
[78] M. M. Coggon *et al.*, "Volatile chemical product emissions enhance ozone and modulate urban chemistry," *Proc. Natl. Acad. Sci. U.S.A.*, vol. 118, no. 32, p. e2026653118, Aug. 2021, https://doi.org/10.1073/pnas.2026653118
[79] C. Zhao *et al.*, "Sensitivity of biogenic volatile organic compounds to land surface parameterizations and vegetation distributions in California," *Geosci. Model Dev.*, vol. 9, no. 5, pp. 1959–1976, May 2016, https://doi.org/10.5194/gmd-9-1959-2016
[80] K. Sun *et al.*, "Vehicle Emissions as an Important Urban Ammonia Source in the United States and China," *Environmental Science*, vol. 51, no. 4, pp. 2472–2481, 2017, https://doi.org/https://doi.org/10.1021/acs.est.6b02805

[81] J. L. Laughner and R. C. Cohen, "Direct observation of changing NOx lifetime in North American cities," *Science*, vol. 366, no. 6466, pp. 723–727, Nov. 2019, https://doi.org/10.1126/science.aax6832

[82] I. Lopez-Coto *et al.*, "Assessment of Planetary Boundary Layer Parameterizations and Urban Heat Island Comparison: Impacts and Implications for Tracer Transport," *Journal of Applied Meteorology and Climatology*, vol. 59, no. 10, pp. 1637–1653, Oct. 2020, https://doi.org/10.1175/JAMC-D-19-0168.1

[83] P. E. Saide *et al.*, "Understanding and improving model representation of aerosol optical properties for a Chinese haze event measured during KORUS-AQ," *Atmos. Chem. Phys.*, vol. 20, no. 11, pp. 6455–6478, Jun. 2020, https://doi.org/10.5194/acp-20-6455-2020

[84] K. R. Travis *et al.*, "Limitations in representation of physical processes prevent successful simulation of $PM_{2.5}$ during KORUS-AQ," *Atmos. Chem. Phys.*, vol. 22, no. 12, pp. 7933–7958, Jun. 2022, https://doi.org/10.5194/acp-22-7933-2022

[85] E. Velasco, A. Retama, M. Zavala, M. Guevara, B. Rappenglück, and L. T. Molina, "Intensive field campaigns as a means for improving scientific knowledge to address urban air pollution," *Atmospheric Environment*, vol. 246, p. 118094, Feb. 2021, https://doi.org/10.1016/j.atmosenv.2020.118094

[86] Molina, Velasco, Retama, and Zavala, "Experience from Integrated Air Quality Management in the Mexico City Metropolitan Area and Singapore," *Atmosphere*, vol. 10, no. 9, p. 512, Aug. 2019, https://doi.org/10.3390/atmos10090512.

[87] L. T. Molina *et al.*, "An overview of the MILAGRO 2006 Campaign: Mexico City emissions and their transport and transformation," *Atmos. Chem. Phys.*, vol. 10, no. 18, pp. 8697–8760, Sep. 2010, https://doi.org/10.5194/acp-10-8697-2010

[88] C. H. Halios and J. F. Barlow, "Observations of the Morning Development of the Urban Boundary Layer Over London, UK, Taken During the ACTUAL Project," *Boundary-Layer Meteorol*, vol. 166, no. 3, pp. 395–422, Mar. 2018, doi: 10.1007/s10546-017-0300-z.

[89] G. L. Mullendore, M. C. Barth, P. M. Klein, and J. H. Crawford, "Field Campaigns with a Broad Impact: Integrating Meteorology and Chemistry", BAMS, vol. 103, iss. 4, Apr 2022, https://doi.org/10.1175/BAMS-D-19-0216.A

[90] H. Tanimoto et al., The greenhouse gas observation mission with Global Observing SATellite for Greenhouse gases and Water cycle (GOSAT-GW): objectives, conceptual framework and scientific contributions, *Prog Earth Planet Sci*, 12, 8, 2025. https://doi.org/10.1186/s40645-025-00684-9

[91] He, J., et al. (2024) COVID-19 perturbation on US air quality and human health impact assessment. PNAS Nexus 3(1).